GREEN SYNTHESIS OF SILVER NANOPARTICLE USING *Curcuma longa* EXTRACT AND ITS' APPLICATION IN HEAVY METAL SENSING AND PHOTOCATALYTIC ACTIVITY

A DISSERTATION SUBMITTED FOR THE PARTIAL FULFILLMENT OF THE REQUIRMENT FOR THE MASTERS OF SCIENCE DEGREE IN CHEMISTRY

By

Asmita Sapkota Upadhaya

Exam Roll. No.: CHE 1705/076

T.U. Regd. No.: 5-2-50-358-2014

CENTRAL DEPARTMENT OF CHEMISTRY

INSTITUTE OF SCIENCE AND TECHNOLOGY

TRIBHUVAN UNIVERSITY, KIRTIPUR, KATHMANDU, NEPAL

July, 2023

BOARD OF EXAMINER AND CERTIFICATE OF APPROVAL

This dissertation entitled by "**Green Synthesis of Silver Nanoparticles Using *Curcuma longa* Extract and It's Application in Heavy Metal Sensing and Photocatalytic Activity**"**,** by **Ms. Asmita Sapkota Upadhaya**, under the supervision of **Dr. Achyut Adhikari,** Central Department of Chemistry, Tribhuvan University, Nepal, is hereby submitted for the partial fulfillment of the Master of Science (M. Sc.) Degree in Chemistry.

……..

Supervisor

Asso. Prof. Dr. Achyut Adhikari

Central Department of Chemistry

Tribhuvan University, Kirtipur, Kathmandu

…….	…..……
Internal Examiner	**External Examiner**
Asst. Prof. Dr. Hari Paudyal	Asst. Prof. Dr. Deval Prasad Bhattarai
Central Department of Chemistry	Amrit Campus
Tribhuvan University	Tribhuvan University
Kirtipur, Kathmandu	Kirtipur, Kathmandu

……..

Head of Department

Prof. Dr. Jagadeesh Bhattarai

Central Department of Chemisty

Tribhuvan University, Kirtipur, Kathmandu

Date: 2023-07-04 (2080/03/19)

RECOMMENDATION

This is to certify that the thesis entitled **"Green Synthesis of Silver Nanoparticles Using *Curcuma longa* Extract and It's Application in Heavy Metal Sensing and Photocatalytic Activity"** submitted to Institute of Science and Technology, Tribhuvan University, for the degree of Master of Science is a bona fide record of research work carried out by Ms. **Asmita Sapkota Upadhaya** in the Central Department of Chemistry, Kirtipur, Kathmandu, Nepal, under my guidance and supervision. To the best of my knowledge, this work has not been submitted to any other degree in this institute.

……..

Supervisor

Dr. Achyut Adhikari

Associate Professor,

Central Department of Chemistry,

Tribhuvan University, Kirtipur, Kathmandu, Nepal

DECLARATION

I, **Asmita Sapkota Upadhaya**, declare that this research was carried out by me and has not been presented either wholly or partly for the award of any degree elsewhere. All sources of scholarly information used in this thesis were duly acknowledged and listed in reference section.

……..

Asmita Sapkota Upadhaya

Central Department of Chemistry,

Tribhuvan University, Kirtipur, Kathmandu, Nepal

Date: 2023-07-04 (2080/03/19)

ACKNOWLEDGMENTS

I manifest my heartfelt gratitude to my adviser Dr. Achyut Adhikari, Associate Professor, Central Department of Chemistry, Tribhuvan University, for his constant guidance, motivation and firm help to face the challenges during my research. I appreciate his unbounded deep scientific insights, optimistic thoughts and research independence provided to me.

I am extremely thankful to Prof. Dr. Jagadeesh Bhattarai, Head of Department, Central Department of Chemistry, Tribhuvan University, for providing me an opportunity to carry out this dissertation. I would like to express my gratitude to all the respected teachers of CDC for their valuable suggestions and inspiration. I am also thankful to all the administrative and laboratory staffs of CDC for their assistance during my laboratory work at CDC.

I express my sincere thanks to National Academy to Science and Technology (NAST), Lalitpur for XRD. I extend my gratitude to Dr. Khagaraj Sharma, Associate Professor, Central Department of Chemistry for FTIR.

Inadequate thought in terms of words and expression, this dissertation owes a lot to my beloved parents and colleagues for their support, suggestions, inspiration, encouragement & good wishes for the success of my dissertation.

Last but not the least I thank every supportive hands that have not been given mentioned by their name but give their invaluable help directly or indirectly throughout the study and soliciting good wishes for my future.

Asmita Sapkota Upadhaya

LIST OF ABBREVIATIONS

Λ	Wavelength
ΔA	Intensity ratio
AgNPs	Silver Nanoparticles
AOP	Advanced Oxidation Species
CB	Conduction Band
CR	Congo Red
CUR	Curcumin
DNA	Deoxyribonucleic Acid
DW	Distilled Water
FCC	Face-centered cubic
FTIR	Fourier Transform-Infrared Spectroscopy
FWHM	Full Width at Half Maximum
JCPDS	Joint Committee On Power Diffraction Standards
keV	Kilo Electron Volt
MO	Methyl Orange
MP	Microprobes
MB	Methylene Blue
Nm	Nano meter
NPs	Nanoparticles
PR	Phenol Red
ROS	Reactive Oxygen Species

Rpm	Revolution per minute
SEM	Scanning Electron Microscopy
SPR	Surface Plasmon Resonance
TEM	Transmission Electron Microscopy
UV-Vis	Ultra Violet Visible
VB	Valence Band
XRD	X-ray Diffraction

ABSTRACT

The green synthesis approach was employed in this study for the preparation of silver nanoparticles (AgNPs) using the aqueous extract of *Curcuma longa* rhizome. The metabolites present in *C. longa* play important role in the reduction of Ag^{+} to Ag^{0} and capping of AgNPs. The confirmation of AgNPs formation was observed through a characteristic SPR band of Ag^{0} at 428 nm in UV-Visible spectroscopy and these were found to be stable for more than 20 days. The AgNPs were face-centered cubic (fcc) crystalline, predicted from the XRD data having an average size of 6.66 nm. The FTIR spectra provided insights into the functional groups present in the extract, which played a role in stabilizing the AgNPs. The strong and wide peak at 3632 cm^{-1} observed in the rhizome extract was significantly weakened in the nanoparticles, suggesting the participation of hydroxyl group (-OH) present in the extract's compounds in the reduction of silver ions. Without modifying the suspension of AgNPs, a colorimetric technique was used for heavy and toxic metal sensing in the aqueous medium. The obtained AgNPs were found to be highly sensitive and selective towards Hg^{2+} ion which can be detected by the naked eye as the AgNPs suspension turned colorless on the addition of 45 µL of 1 mM Hg^{2+}. The photocatalytic property of synthesized AgNPs was observed towards the organic dyes, and it also demonstrated sensing capabilities for formaldehyde. These results suggest an application of AgNPs influenced by *Curcuma longa* for degradation of dyes and metal sensing.

Keywords: Green synthesis, Nanoparticle, Silver nanoparticle, Mercury sensor, Sensing, Photocatalytic activity, Degradation

TABLE OF CONTENTS

BOARD OF EXAMINER AND CERTIFICATE OF APPROVAL ii

RECOMMENDATION iii

DECLARATION iv

ACKNOWLEDGMENTS v

LIST OF ABBREVIATIONS vi

ABSTRACT viii

TABLE OF CONTENTS ix

LIST OF FIGURES xiii

LIST OF TABLES xv

CHAPTER I 1

1 INTRODUCTION 1

1.1 Introduction of Nanoparticle 1

1.2. Classification of Nanoparticles 2

1.3 Synthesis of Nanoparticles 3

1.3.1 Need for Green Synthesis 4

1.4 Importance of Nanomaterials 4

1.5 Silver Nanoparticles 5

1.5.1 Why Silver Nanoparticle? 5

1.5.2 Fabrication of AgNPs 6

1.5 3. Protocols for the Biosynthesis of AgNPs 7

1.5.3.1 From Plant Extract 7

1.5.3.2 From Microbes 8

1.6 Characterization of Silver Nanoparticles 8
1.6.1 UV-Visible Spectroscopy 8
1.6.2 X-Ray Diffraction (XRD) 9
1.6.3 Dynamic Light Scattering 10
1.6.4 Fourier Transform Infrared (FTIR) Spectroscopy 10
1.6.5 X-Ray Photoelectron Spectroscopy (XPS) 11
1.6.6 Scanning Electron Microscopy 12
1.6.7 Transmission Electron Microscopy 12
1.7 Applications of AgNPs 12
1.7.1 Detection of Metal Ions 13
1.7.2 Silver Nanoparticles as Antibacterial Agents 14
1.7.3 Photocatalytic Activity 15
1.8 Objective of the Study 17
1.8.1 General Objective 17
1.8.2 Specific Objectives 17
CHAPTER II 18
2 LITERATURE REVIEW 18
2.1 Plant Description 18
2.2 History of Nanomaterials 19
2.3 Research Gap 25
CHAPTER III 26
3 MATERIALS AND METHODS 26
3.1 Materials 26
3.1.1 Chemicals 26

3.1.2 Plant Material 26
3.2 Biosynthesis of AgNPs 27
3.2.1 Preparation of Plant Extract 27
3.2.2 Preparation of Silver Nitrate Solution 27
3.2.3 Biosynthesis of AgNPs 28
3.2.4 Purification of AgNPs 28
3.3 Characterization Techniques 28
3.3.1 UV-Vis Spectroscopy 28
3.3.2 Fourier Transform Infra-Red (FTIR) 28
3.3.3 X-ray Diffraction (XRD) 29
3.4 Metal Sensing Activity of AgNPs 30
3.4.1 Preparation of Metal Salt Solution 30
3.4.2 Metal Colorimetric Sensing 31
3.5 Dye Degradation Assay 31
3.6 Detection of Formaldehyde Solution 32
3.7 Data Analysis 32
CHAPTER IV 33
4 RESULTS AND DISCUSSION 33
4.1 Green synthesis of AgNPs 33
4.2 Characterization of AgNPs 34
4.2.1 UV-Vis Spectrometry 34
4.2.2: X-Ray Diffraction 35
4.2.3 Study of Biomolecular Reduction by FTIR 36
4.3 Application of Synthesized AgNPs in Analysis 38

4.3.1 Colorimetric Sensing of AgNPs 38

4.3.1.1 Sensitivity of AgNPs towards Hg^{2+} Ions 40

4.3.2 Photocatalytic Degradation of Methylene Blue 43

4.3.3 Photocatalytic Degradation of Methyl Orange (MO) 45

4.3.4 Detection of Formaldehyde 47

CHAPTER V 50

5 CONCLUSION 50

REFERENCES 51

APPENDIX 79

LIST OF FIGURES

Figure 1.1: Different approaches of synthesis to the silver nanoparticles.....4

Figure 1.2: Synthesis from the top-down and bottom-up of nano fabrication.....7

Figure 1.3: Applications of AgNPs.....13

Figure 1.4: Visual summary of several phenomena affecting AgNps dissolution 15

Figure 1.5: Photocatalytic degradation of dyes 17

Figure 2.1: Curcuma longa 18

Figure 2.2: Yearly publications on green silver nanoparticle production from 2001 to 2019.....21

Figure 3.1 : Powder of Curcuma longa rhizome.....26

Figure 3.2: Schematic representation of various steps involved in the execution of experiments 29

Figure 4.1 : Colour change during the synthesis of AgNPs nanoparticles 33

Figure 4.2 : UV-visible absorption spectra of Curcuma longa at different time 24 hr, 48 hr and 20 days.....35

Figure 4.3: XRD patterns of *Curcuma longa* mediated AgNPs 35

Figure 4.4: FTIR spectra of: (A) Curcuma longa extract (B) AgNPs.....38

Figure 4.5: Color change of nanoparticle dispersion after the addition of the metal solution.....39

Figure 4.6: UV-Vis spectra of Silver NPs dissolution with various metal ions. 40

Figure 4.7: Color change on the addition of (A) 20-800 µL of Hg^{2+} (B) 25-80 µL of Hg^{2+} 41

Figure 4.8: UV-Vis Spectra of Silver nanoparticles with (A) 20-800 µL of Hg^{2+} (B) 25-80µL of Hg^{2+} 42

Figure 4.9: UV-Vis absorption at different time of methylene blue in presence of AgNPs 45

Figure 4.10: Graphical representation of degradation of methylene blue by AgNPs . 45

Figure 4.11: UV-Vis absorption at different times of methyl orange in the presence of AgNPs 47

Figure 4.12: Graphical representation methyl orange degradation by AgNPs 48

Figure 4.13: UV spectra of different percentage concentration solutions of formaldehyde with AgNPs 50

LIST OF TABLES

Table 2.1: Various rhizomes extract used for the green synthesis of AgNPs 23

Table 3.1**:** The amount of metal salt required for the experiment 30

Table 4.1: Calculation of size of IONPs 36

Table 4.2**:** Calculation of methylene blue dye degradation efficiency by synthesized AgNPs 44

Table 4.3**:** Calculation of degradation efficiency of methyl orange by synthesized AgNPs 47

CHAPTER I

1 INTRODUCTION

1.1 Introduction of Nanoparticle

In the current scenario, Nanotechnology is attracting a lot of attention as an emerging field of research focused on the progress of nanomaterials and nanoparticles for usage in numerous industries, including catalysis, electrochemistry, biomedicine, pharmaceuticals, sensors, food technology, cosmetics, etc. In the last few years, a new word in the world of nanoparticles, metal nanoparticles has emerged. Metallic nanoparticles are created from noble metals like gold, silver, and platinum that have beneficial effects on health and are used in the production of nanoparticles (Bhattacharya & Mukherjee, 2008). Because of their unique properties that are beneficial for catalysis, composite-like polymer preparations (Moura et al., 2017), disease diagnosis and treatment (Banerjee et al., 2017), sensor technology (Gomez-Romero, 2001; Królikowska et al., 2003) and electronic magnetic properties and antimicrobial activities (Królikowska et al., 2003; Zhao & Stevens, 1998). Researchers are currently concentrating on the synthesis of nanomaterials, nanostructures, and metal nanoparticles.

In specific applications in the medical, commercial, and ecological fields, nanoparticles exhibit physicochemical properties that produce unique electrical, mechanical, optical, and imaging capabilities that are highly wanted (Dong et al., 2014; Ma, 2003; Todescato et al., 2016). Additionally, they have reported on the applications for optical, florescence, and photocatalytic activities (Olteanu et al., 2016; Rogozea et al., 2016) used in an array of physical, biological, biomedical, and pharmaceutical sectors (Królikowska et al., 2003).

Nanoparticles are a diverse class of materials that contain substances that are particulate and have a dimension of at least 10 nm and less than 100 nm (Laurent et al., 2010). NPs are distinctive and make suitable choices for a variety of applications, including thermal properties, mechanical properties, magnetic properties, and electronic and optical properties. These physicochemical qualities include huge surface area, mechanical strength, optical activity, and chemical reactivity. Manufactured

nanoparticles may have practical applications in several fields, including medicine, engineering, catalysis, and environmental remediation. This is because of their special material properties and submicroscopic size.

Due to its innovative developments and numerous uses in the current environment, the area of nanotechnology is growing rapidly and is becoming increasingly important. Due to their distinctive physiochemical features, such as their catalytic, optical, electronic, magnetic, and antibacterial activities, metal nanoparticles have received substantial study. Additionally, they have a large specific surface area and a more surface atom content (Królikowska et al., 2003; Zhao & Stevens, 1998). Nanoparticles disclose size- and shape-dependent properties that are of interest for applications vary from biosensing and catalysts to optics, antibacterial activity, computer transistors, electrometers, chemical sensors, wireless electronic logic, and memory systems (Lee et al., 2008; Tang et al., 2006). These particles have numerous uses in a variety of industries, including medical imaging, nanocomposites, filtration, drug delivery, and tumor hyperthermia (Panigrahi et al., 2004; Pissuwan et al., 2006). Unique physiochemical characteristics of NPs include their surface area, strong reactivity, variable pore size, and distinctive particle shape (Siddiqui et al., 2015).

Nanomaterials are defined as substances with organized components that have at least one dimension smaller than 100 nm. Because of their extremely numerous size and great surface to-volume ratio, nanoparticles have variety of physiochemical characteristics than bulk materials with the similar chemical composition. These variations include melting point, optical absorption, thermal conductivity, biological and satire qualities, photocatalytic activity, and mechanical, biological, and satirical properties.

1.2. Classification of Nanoparticles

Since nanoparticles may exhibit spherical, tubular, or irregular shapes as well as exist in fused, aggregated, or agglomerated forms, they can be categorized according to their dimensions, morphology, composition, uniformity, and agglomeration.

Siegel classified nanostructured materials dimensionality into the following four categories: (Buzea et al., 2007)

i. Zero dimensional (0D) nanoclusters

ii. One-dimensional (1D) multilayers

iii. Two-dimensional (2D) nanograined layers

iv. Three-dimensional (3D) equiaxed bulk solids

Based on chemical composition, nanoparticles are mainly divided into two categories.

i. Organic nanoparticles which contains carbon NPs (fullerenes)
ii. Inorganic nanoparticles which contains noble metal NPs (silver, gold, copper etc.), semiconductor NPs (Zinc oxide, titanium oxide etc.), and magnetic NPs.

Based on their source of origin and synthesis, nanoparticles can be categorized into two types.

i. Natural NPs (synthesized by natural processes)
ii. Engineered NPs (synthesized in lab) (Lidén, 2011)

1.3 Synthesis of Nanoparticles

Both top-down and bottom-up methods can be used for the synthesis of nanomaterials. Top-down synthesis uses chemical, physical, or biological energy to break down larger structures into smaller ones. In order to generate a massive nanostructure, bottom-up synthesis uses various chemical, physical, or biological events that start at the atomic level (Das et al., 2017). This approach is mostly used to construct nanostructured carriers (NC) using chemical and biological techniques.

For the synthesis of NPs, a wide range of physical and chemical techniques have been researched, which includes laser ablation, pyrolysis, chemical or physical vapor deposition, lithography, electro-deposition, sol-gel, etc. These techniques are either costly or use hazardous materials, for example- organic solvents and toxic reducing agents (Choi & Park, 2011). Green methods for synthesis have been created to avoid potentially hazardous chemicals. These techniques have generated a lot of interest because they are ecofriendly, rapid, facile, and energy-efficient. The biological method seems to be an excellent match in the present situation. To synthesize silver nanoparticles, natural materials which include plants (Gardea-Torresdey et al., 2002) , bacteria (Joerger et al., 2000), fungi (Bhainsa & D'Souza, 2006), and yeast are employed.

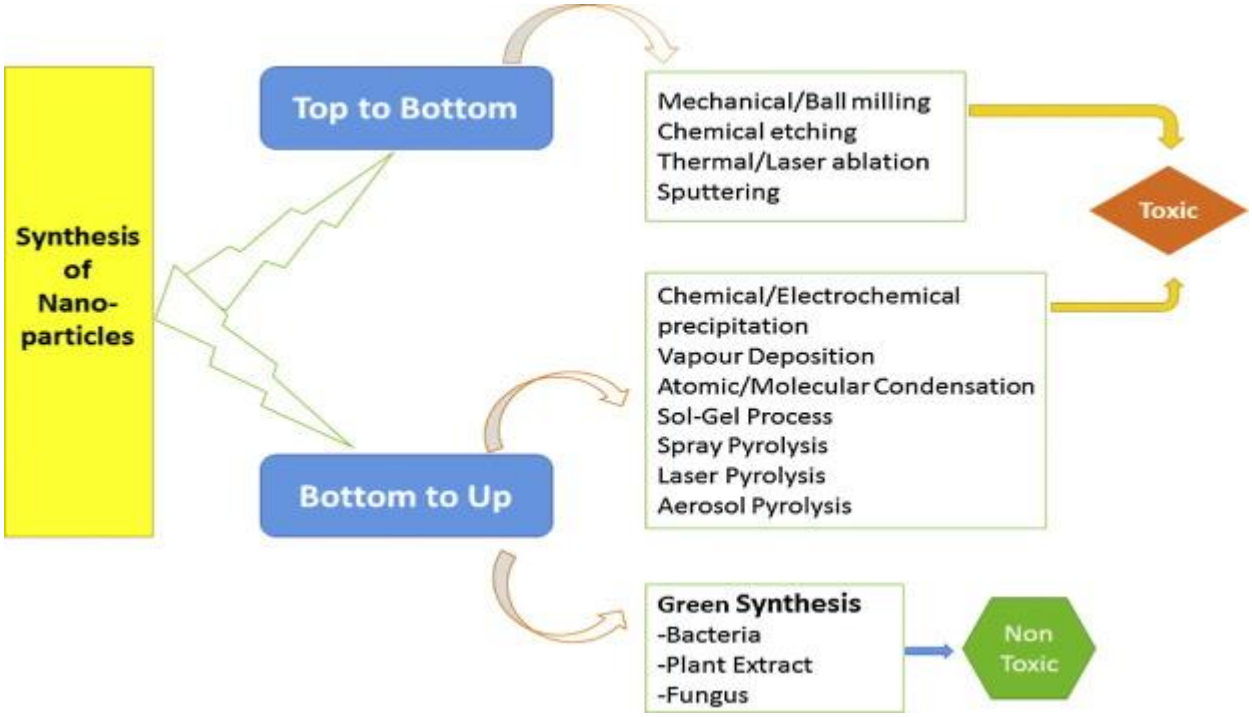

Figure 1.1: Different approaches of synthesis to the silver nanoparticles

(Ahmad, et al., 2016a)

1.3.1 Need for Green Synthesis

The major reaction that takes place during the biosynthesis of nanoparticles is reduction/oxidation. The high expenses of the physical and chemical techniques increased the requirement for the biosynthesis of nanoparticles. This is not a concern for biosynthesized nanoparticles produced using green synthesis (Begum et al., 2009). Green synthesis is an advancement over chemical and physical methods because it is more convenient to scale up for large-scale synthesis, less expensive, and more environmentally friendly. It also reduced the need for harmful chemicals, high pressure, energy, and temperature (Kouvaris et al., 2012; Song & Kim, 2009). As a result, experiments to create NPs using biological techniques were made, and they were successful, benefiting the field of nanotechnology.

1.4 Importance of Nanomaterials

The properties that result as particle size decreases from milli to micro to nano are better than those of conventional materials. Large surface atom and surface energy fractions may have an impact on the mechanical, thermal, and catalytic properties of

nanomaterials. Compared to their bulk materials, the increased surface area to volume ratio causes crystal defects to exhibit lower melting points (Buffat & Borel, 1976) and higher mechanical strengths. Thus, more and more potential applications of nanomaterials are being discovered.

1.5 Silver Nanoparticles

Silver is a soft, white, glossy element that is not soluble in water. The good therapeutic capabilities of silver have made it one of the most well-known metallic nanoparticles since ancient times. The AgNPs are beneficial for biological detection and imaging (Jain et al., 2008) because they have significant optical characteristics. Silver nanoparticles (AgNPs) have been utilized extensively in the production of creams, food packaging and preservation systems, water purification systems, electronics, household goods, ointments, and medical implants. (Silver, 2003). Finely scattered metallic silver exhibits special qualities like chemical stability, excellent electrical conductivity and catalytic activity, as well as other more specialized ones like anti bacteriostatic effects and non-linear optical behavior, among others. Because of the simplicity of their manufacture and chemical changes, AgNPs are special in nanoscale systems. In the disciplines of electronics, material sciences, and medical, AgNPs are used in the development of new technology. AgNPs are the subject of greater research globally due to its broad variety of applications.

A rare combination of valuable properties, including high electrical double-layer capacitance, catalytic activity, well-developed surfaces, and unique optical properties associated with the Surface Plasmon Resonance (SPR), are present in silver nanoparticles, according to fundamental studies carried out over the past three decades. As a result, they are utilized as a component in the creation of new electrical, optical, and sensor technologies.

1.5.1 Why Silver Nanoparticle?

One of the fundamental elements that naturally occur on our planet is silver. Many disorders, including mental illness, epilepsy, nicotine addiction, gastroenteritis, and infectious diseases including syphilis and gonorrhea, have been treated with the aid of soluble silver compounds like silver slats. Metallic silver seems to have little negative effects on health, however soluble silver complexes can be dangerous since they are

more easily absorbed. Metallic silver appears to pose minimal risk, even though the presence of free silver ions determines the acute toxicity of silver in the environment. The immune, cardiovascular, neurological, or reproductive systems are not thought to be harmed by silver in any form, and it is not considered to be carcinogenic (Drake & Hazelwood, 2005). As these technology and goods spread throughout the global economy, silver demand will probably increase as it finds new applications, particularly in the textile, plastics, and medical factories, altering the pattern of Ag emission (Furst & Schlauder, 1978)

The creation of lotions, food packaging and preservation, water purification systems, electronics, household products, ointments, and medical implants has all made extensive use of silver nanoparticles (Silver, 2003). Ag is among all metallic nanoparticles well known due to its exceptional therapeutic qualities since ancient times. The use of AgNPs in biological imaging and detection is advantageous (Jain et al., 2008) because they have significant optical characteristics.

1.5.2 Fabrication of AgNPs

In addition to naturally occurring nanomaterial, "top-down" and "bottom-up" approaches are currently used to create nanoparticles. These strategies were created as a result of Feynman's address to the American Physical Society in 1959.

i. Top-down approach: Bulk material is fragmented to yield the particle at the nanoscale
ii. Bottom-up approach: To create nanostructured materials, individual atoms and molecules are brought together or self-assembled.

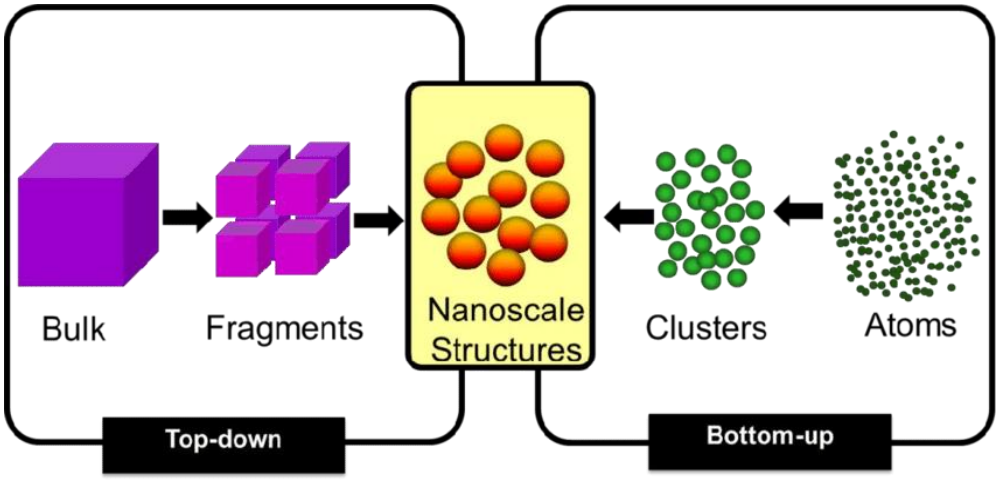

Figure 1.2*:* Synthesis from the top-down and bottom-up of nano fabrication.

(Rawat, 2015)

1.5 3. Protocols for the Biosynthesis of AgNPs

AgNPs are generated by a simple, one-step process that does not produce harmful or expensive chemicals, making them safe, inexpensive, and environmentally friendly. Recent years have included intense research into the biosynthesis of AgNPs of various sizes, shapes, levels of stability, and antibacterial activity in both plants and microorganisms (Vanlalveni et al., 2021).

1.5.3.1 From Plant Extract

Many different plant parts, including leaves, roots, flowers, rhizomes, etc., have been effectively used to produce AgNPs (Ahmad et al., 2017; Erenler et al., 2021; Sumitha et al., 2018). To eliminate trash and other unwanted materials, various plant parts are gathered from various sources, properly cleaned with tap water, and then washed once more with distilled water. The sections are then used to manufacture the extract after being dried and crushed to make powder. As continuous high-temperature heating may cause the phytochemicals in the biomass extract to degrade, the chopped or crushed plant parts are normally heated below 60 °C for a brief period to create the extract. AgNPs were created by adding plant extracts with various pH levels while heating solutions with variable concentrations of Ag salt as a metal precursor at various temperatures (Ajitha et al., 2015; Ali et al., 2015; Dhand et al., 2016). The biomaterials in the extract prevent the need for chemical stabilizers by serving as both a reducing agent and a stabilizing agent for the synthesis of AgNPs (Biswas et al., 2018;

Manikandan et al., 2015). Visual color changes or UV-Vis spectroscopy can be used to monitor the growth of AgNPs. The latter clearly shows a significant peak caused by the surface plasmon resonance (SPR) of AgNPs at around 430-450 nm (Biswas et al., 2018). Once the AgNPs have been properly mediated, the mixture is centrifuged at a high rpm to separate the NPs, followed by suitable solvent washing and drying in a low-temperature oven (Kathiraven et al., 2015; Kokila et al., 2015).

1.5.3.2 From Microbes

Today, it has been proven to be a great technique to use microbial cells to produce metal nanoparticles. Excellent biofactories for manufacturing AgNPs can be found in the cells of microorganisms (Jha et al., 2009; Vigneshwaran et al., 2007). As a suspension in sterile, distilled water that also contains the culture medium, the cultures are initially permitted to grow and develop. The precursor of AgNPs is then added to the cultivated microbe in varying concentrations, followed by continuous mechanical stirring in the dark. A UV-Vis spectrophotometer is used to track the reaction's expansion. To separate the created AgNPs, the mixture is centrifuged for 10 to 15 minutes at a speed of around 3000 rpm (Ahmad, et al., 2016b; Shivaji et al., 2011).

1.6 Characterization of Silver Nanoparticles

Nanoparticle's behavior, bio-distribution, safety, and efficacy are significantly influenced by their physicochemical characteristics. To ascertain the beneficial properties of the produced particles, AgNP characterization has therefore become crucial. The materials are characterized using a variety of analytical techniques, including scanning electron microscopy (SEM), transmission electron microscopy (TEM), X-ray diffractometry (XRD), Fourier transform infrared spectroscopy (FTIR), dynamic light scattering (DLS), and atomic force microscopy (AFM).

1.6.1 UV-Visible Spectroscopy

UV-Vis spectroscopy is a very beneficial and reliable method for the initial characterisation of produced nanoparticles. It is also employed to monitor AgNP production and stability (Sastry et al., 1998). AgNPs strongly interact with specific light wavelengths because of their unique optical properties. Finally, UV-Vis spectroscopy does not require calibration to characterize the particles in colloidal suspensions because it is quick, simple, sensitive, selective for different types of NPs, and only takes

a short period of time for quantification. UV-Vis spectroscopy is a very beneficial and reliable method for the initial characterization of produced nanoparticles. It is also employed to monitor AgNP production and stability (Huang et al., 2007; Leung et al., 2006; Noginov et al., 2007; Taleb et al., 1998; Tomaszewska et al., 2013). The valence band and conduction band, in which electrons can freely flow, are relatively near to one another in AgNPs. A surface plasmon resonance (SPR) absorption band is created as a result of the free electrons in the silver nanoparticles collectively oscillating in resonance with the light wave. Depending on the size of the particles, the dielectric medium, and the chemical environment, AgNPs absorb differently (He et al., 2002; Link & El-Sayed, 2003; Taleb et al., 1998). It is well known that this peak, which is related to a surface plasmon, may be observed for different metal nanoparticles with sizes ranging from 1 to 100 nm (Henglein, 1993; Sastry et al., 1997, 1998). Over the course of more than a year, biologically created AgNPs were examined, and UV-Vis spectroscopy was used to locate an SPR peak at the same wavelength.

1.6.2 X-Ray Diffraction (XRD)

The popular analytical method known as X-ray diffraction (XRD) has been used to examine crystal and molecular structures (Leung et al., 2006), qualitatively identify different chemicals and exhibit the physico-chemical and structural properties of the sample. Thus, XRD can be used to examine the structural properties of a wide range of materials, including inorganic catalysts, superconductors, biomolecules, glasses, polymers, and more (Macaluso, 2009). The investigation of these materials requires the use of diffraction patterns. By contrasting the diffracted beams with the reference database stored in the Joint Committee on Powder Diffraction Standards (JCPDS) libraryc, 2010), Quantitative chemical species resolution, crystallinity assessment, isomorphous substitution detection, molecular size measurements, and more have all been done (Ananias et al., 2013; Dey et al., 2009). A multitude of diffraction patterns, which are illustrations of the physico-chemical characteristics of the crystal formations, are created when an X-ray reflection is reflected off of any crystal. Each substance has a unique diffraction beam, which makes it feasible to characterize and distinguish each substance. Diffracted beams normally come from a powder specimen. The purity or impurity of the sample materials can also be seen in the diffracted patterns. As a result, XRD has been used to define and identify the materials of forensic samples, industrial samples, and geological sample materials for a very long time (Cassie & Baxter, 1944;

Dolatmoradi et al., 2013; A. Khan et al., 2013; Kou et al., 2012; Pavlidou & Papaspyrides, 2008; Sinha Ray & Okamoto, 2003; Vaia & Liu, 2002; Yazdian et al., 2013; Zawrah et al., 2013).

1.6.3 Dynamic Light Scattering

The physicochemical characterization of synthesized nanomaterials is crucial for the evaluation of biological activities using radiation scattering techniques (Inagaki et al., 2013; Lin et al., 2014a; Sapsford et al., 2011). A surface measuring between a submicron and 1 nanometer can be used by DLS to investigate the size distribution of microscopic particles in solution or suspension (Lin et al., 2014a; Sapsford et al., 2011). A technique that depends on light and particle interaction is dynamic light scattering. This technique can be applied to measure narrow molecule size distributions, particularly those between 2 and 500 nm (Tomaszewska et al., 2013). DLS is the method most frequently utilized for the characterization of nanoparticles (Jans et al., 2009; Khlebtsov & Khlebtsov, 2011; Zanetti-Ramos et al., 2009). To quantify the light scattered from a laser that passes through a colloid, DLS largely relies on Rayleigh scattering from the suspended nanoparticles (Fissan et al., 2014). Then, by examining the modulation of the scattered light intensity as a function of time, the hydrodynamic size of the particles may be determined (Dieckmann et al., 2009; Koppel, 2003). Any nanomaterial must be characterized in solution to be judged for its hazardous potential. As a result, DLS is mostly employed for determining particle size and size distributions in physiological or aqueous solutions (Murdock et al., 2008). Typically, DLS yields bigger sizes than TEM, which may be explained by Brownian motion. DLS is a nondestructive technique used to determine the average diameter of nanoparticles dissolving in liquids. It has the unique benefit of investigating numerous particles at once, but it consists a variety of sample-specific drawbacks (Kou et al., 2012; Lange, 1995).

1.6.4 Fourier Transform Infrared (FTIR) Spectroscopy

With FTIR, we may obtain accuracy, consistency, and a great signal-to-noise ratio. Using FTIR spectroscopy, which allows for the detection of minute absorbance variations on the scale of nanometers, it is able to discriminate between the small absorption bands of functionally active residues and the vast framework absorption of the entire protein while doing difference spectroscopy (Gerwert, 1999; Jung, 2000; S.

Kim & Barry, 2001, 2001; Mäntele et al., 1988; Vogel & Siebert, 2000). In academic and commercial research, In order to determine whether biomolecules are involved in the formation of nanoparticles, FTIR spectroscopy is regularly used (Lin et al., 2014b; Perevedentseva et al., 2010; Shang et al., 2007). The study of nano-scaled materials has also benefited from the expansion of FTIR, as demonstrated by the discovery of functional molecules covalently transferred to gold, silver, graphene, and carbon nanoparticles, as well as the combination of an enzyme and a substrate in a catalytic reaction (Barth & Zscherp, 2002; Baudot et al., 2010). It is also a non-intrusive technique. Last but not least, benefits of FTIR spectrometers over dispersive ones include rapid data gathering, a strong signal, a good signal-to-noise ratio, and reduced sample heating (Kumar & Barth, 2010). A recent advancement in FTIR technology is called attenuated total reflection (ATR)-FTIR spectroscopy (Goormaghtigh et al., 1999; Harrick & Beckmann, 1974; Hind et al., 2001). The chemical characteristics of the polymer plane can be identified using ATR-FTIR, and Compared to traditional FTIR, sample preparation is easier (Kazarian & Chan, 2006; Lin et al., 2014c; Liu & Webster, 2007). How biological molecules contribute to the process that turns silver nitrate into silver can be determined using FTIR, which is a useful, practical, non-invasive, affordable, and simple method.

1.6.5 X-Ray Photoelectron Spectroscopy (XPS)

The value of an empirical formula can be calculated by the quantitative spectroscopic surface chemical analysis technique called XPS (Acosta et al., 2005; Manna et al., 2001) ESCA, or electron spectroscopy for chemical analysis, is another name for XPS. XPS serves a distinct function in providing access to qualitative, quantitative, and speciation knowledge on the sensor surface (Desimoni & Brunetti, 2015). A high vacuum is used for XPS operations. When a nanomaterial is exposed to X-rays, electrons are released, and the amount and kinetic energy of these released electrons are measured to produce an XPS spectrum (Acosta et al., 2005; Manna et al., 2001). Kinetic energy can be used to compute the binding energy. P=S, aromatic rings, C-O, and C=O are all starburst macromolecules that can be recognized and explained using XPS.

1.6.6 Scanning Electron Microscopy

To understand further about nanomaterials, various high-resolution microscopy techniques have recently been developed with the help of the fields of nanoscience and nanotechnology (Wang, 2000). These techniques use a beam of extremely powerful electrons to study objects at extremely fine scales. SEM is a surface imaging technique for electron microscopy that is completely able of resolving varied molecule sizes, size distributions, forms of nanomaterials, and the micro- and nanoscale surface morphology of the produced particles (Fissan et al., 2014; Hall et al., 2007; Lin et al., 2014a). By manually counting and measuring the particles or by utilizing specialized software, we may utilize SEM to evaluate the morphology of the particles and generate a histogram from the images (Fissan et al., 2014). Using SEM and energy-dispersive X-ray spectroscopy (EDX), silver powder's shape and chemical composition can be investigated. SEM has the drawback of not being capable to resolve interior structure, but it can still offer useful insight into the purity and level of molecule aggregation. To determine the morphology of nanoparticles smaller than 10 nm, contemporary high-resolution SEM is used.

1.6.7 Transmission Electron Microscopy

The useful, popular, and relevant TEM technique for the characterization of nanomaterials can be used to quantitatively assess molecule and/or grain size, size distribution, and shape (Lin et al., 2014c; Williams & Carter, 1996). The magnification of TEM is significantly influenced by the distance between the objective lens and the sample as well as the length between the objective lens and its image plane (Williams & Carter, 1996). Compared to SEM, TEM has two advantages: higher spatial resolution and the ability to perform more analytical researches (Hall et al., 2007; Lin et al., 2014c; Williams & Carter, 1996). The necessity for a strong vacuum and thin sample sections are two limitations of TEM (Hall et al., 2007; Lin et al., 2014c), as well as the necessity of lengthy sample preparation. Therefore, to provide the best photos possible, sample preparation is crucial.

1.7 Applications of AgNPs

Applications for AgNPs are numerous and include biomedical research, food preservation, home appliances, and the healthcare sector. The various applications of

AgNPs have gotten their own book reviews and chapters. The primary topic of this article is the use of AgNPs in many biological and therapeutic applications, including antibacterial, antifungal, antiviral, anti-inflammatory, anti-cancer, and anti-angiogenic. Here, we especially discussed earlier seminal works and concluded with current research. Figure presents a schematic diagram for a range of AgNPs applications (Zhang et al., 2016).

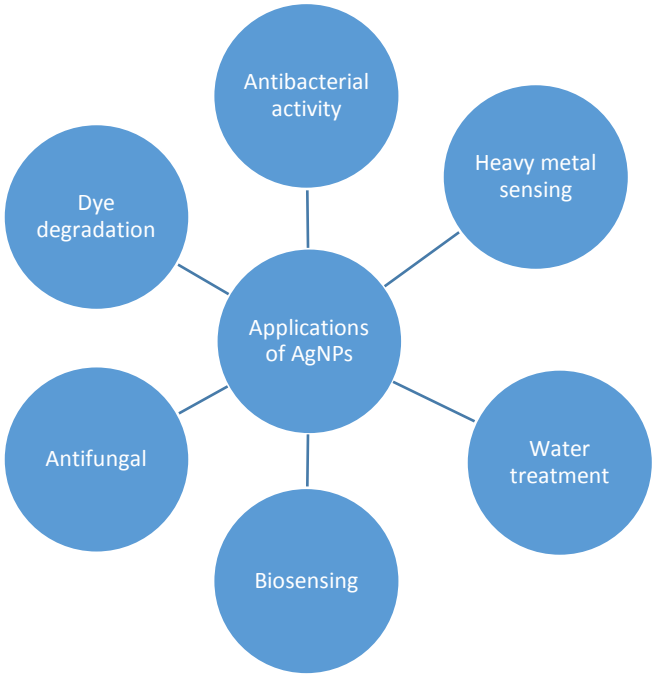

Figure 1.3: Applications of AgNPs

1.7.1 Detection of Metal Ions

The identification of these substances is crucial because heavy metal toxicity is one of the biggest risks to all living things. Various instrumental analytical techniques can be used to determine the amount of heavy and hazardous metals in various materials. The most frequently used techniques are capillary electrophoresis (CE), X-ray fluorescence spectroscopy (XFS), microprobes (MP), inductively coupled plasma/atomic emission spectrometry (ICP-AES), inductively coupled plasma-mass spectroscopy (ICP-MS), ion chromatography ultraviolet-visible spectroscopy (IC-UV-Vis), and atomic absorption spectroscopy (AAS) (Hoang et al., 2013; Li et al., 2013; Yuan et al., 2013).

Although analytical methods are the preferred approaches for the detection of different macromolecules, it would be beneficial to develop methods for the selective naked-eye detection of metal ions in aqueous environments that do not call for a particular

apparatus, particularly for field testing (Yoosaf et al., 2007). Due to the dependence of the plasmon shift on chemical environment around the AgNPs, the sensing of metal ions is based on the surface plasmon resonance (SPR) of AgNPs (Hamad et al., 2014). Furthermore, homogeneous nanoparticle size & shape are not necessary for SPR when used with colorimetric sensors (Yoosaf et al., 2007).

1.7.2 Silver Nanoparticles as Antibacterial Agents

The pathogenic microbes are capable of causing a variety of diseases and are continually evolving with a diverse genetic makeup (Kyriacou et al., 2004). Although there are several commercially accessible antibiotic medicines, using traditional therapy caused these harmful bacteria to develop resistance (Kim et al., 2007).

AgNPs are among the most potent materials and display unique properties (electronic, magnetic, and optical) as a result of their elevated specific surface area and large number of atoms that can interconnect with the environment. These beneficial properties also encourage the production of reactive oxygen. Research in the area of applied nanotechnology has increased as a result of the rise in bacterial resistance to metallic ions and traditional antibiotics (Ouda, 2014).

The AgNPs have a lot of potential against a variety of gram-negative, gram-positive, and antibiotic-resistant bacterial strains, as is well documented (Kim et al., 2007). Low particle sizes and low concentrations of antimicrobial agents can kill bacterial strains. This is coupled with the advantage of demonstrating decreased toxicity to human health and the environment in the case of nanoparticles made through green synthesis, sparking strong interest in their development to combat pathogenic microorganisms (Khan et al., 2019).

The antibacterial activity of AgNPs via pathogenic bacteria involves two different mechanisms of action: the first one (i) involves the nanoparticles adhering to and piercing the bacterial cell membrane, altering it (due to interactions of silver ions with proteins and phosphorous within the cell, preventing the electron transport), and the second one (ii) The bacterial cell wall is involved (as a result of the interlinkage of silver ions with sulfur and phosphorus). AgNPs are designed particularly to assault a number of targets present in germs, including proteins, thiol groups, and cellular walls. Bacteria are often unable to build resistance to AgNPs (MubarakAli et al., 2011).

Depending on their physicochemical properties, AgNPs have a significant potential for usage as antibacterial agents. Because of their combined effectiveness against pathogenic microbes, low production costs, and superior thermal and radiation durability (UV and visible), AgNPs are the potential in biomedical applications to minimize infections.

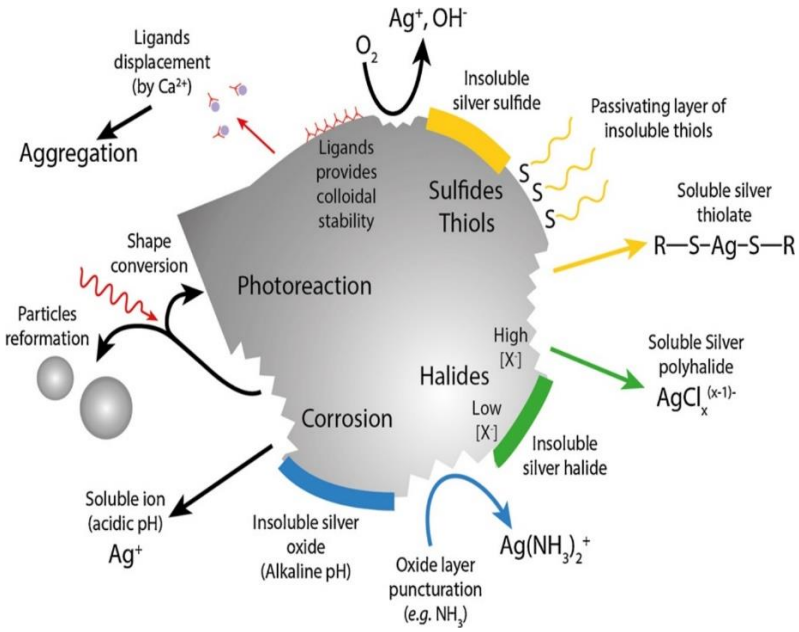

Figure 1.4: Visual summary of several phenomena affecting AgNps dissolution

(Le Ouay & Stellacci, 2015)

1.7.3 Photocatalytic Activity

One Advanced Oxidation Process (AOP) that is helpful in the destruction of different pollutants, including colors, medicines, pesticides, herbicides, hydrocarbons, and the inactivation of microorganisms, is photocatalysis. It has a broad range of uses in wastewater treatment because it may activate a metal-based photocatalyst (typically a semiconductor) using either UV or visible light to enhance oxi-reduction activities on the catalytic surface (Díez et al., 2018). In this first phase, an electron enters the semiconductor's conduction band (CB) from the valence band (VB), where it creates an electron-hole pair (e^+_{CB} and h^+_{VB}) (Gonçalves et al., 2019). Additionally, the production of reactive oxygen species (ROS) in this process is made easier by the water molecules and dissolved oxygen (Carvalho Oliveira Cambrussi et al., 2019).

As a result, ROS (mostly $HO^{\bullet}$ and $O2^{-\bullet}$) have a propensity to react non-selectively and mineralize any organic matter (Žerjav et al., 2020). Therefore, through redox processes, heterogeneous photocatalysis reduces or oxidizes organic molecules when exposed to light. After being exposed to band gap light, the catalyst surface produces electron-hole pairs that serve as an activator for these reactions (Gaya & Abdullah, 2008).

Supported,

$AgNPs + hv \longrightarrow e^-_{CB} + h^+_{VB}$	------	E_1
$O_2 + e^-_{CB} \longrightarrow O_2^-$	------	E_2
$h^+_{VB} + H_2O \longrightarrow HO^{\cdot} + H^+$	------	E_3
$e^-_{CB} + h^+_{VB} \longrightarrow$ heat loss	------	E_4
$HO^{\cdot} + HO^{\cdot} \longrightarrow H_2O_2$	------	E_5
$O_2.^- + H_2O_2 \longrightarrow HO^{\cdot} + OH^- + O_2$	------	E_6
$O_2.^- + H^+ \longrightarrow HOO^{\cdot}$	------	E_7
$HO^{\cdot}$ + organic matter $O_2 \longrightarrow CO_2 + H_2O$	------	E_8

As a result, Eq. (1) depicts the activation of a semiconductor-based metal photocatalyst that produces an electron-hole pair. Organic matter degradation is caused by ROS production, which is referred to in equations (2), (3), (6), and (7). The process results in unwanted recombination in equations (4) and (5). Eq. (4) denotes the spontaneous process of electron-hole pair recombination which reduces the effectiveness of photocatalytic degradation, and Eq. (5) denotes the formation of hydrogen peroxide. For the hydroxyl radicals to oxidize the organic substance, Eq. (8) is valid. The main benefit of AgNPs is that organic chemicals are destroyed during treatment rather than being transported from one phase to another, as is the case with some traditional homogenous treatment procedures.

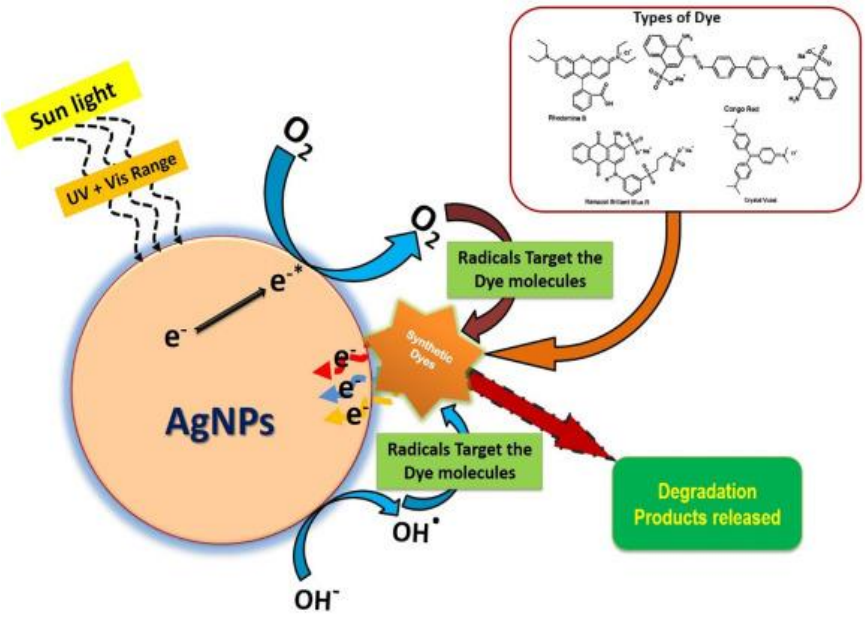

Figure 1.5*:* Photocatalytic degradation of dyes

(Marimuthu et al., 2020)

In the current research, low-cost ecofriendly AgNPs were mediated by using the *Curcuma longa.* The colorimetric sensing ability towards heavy metals, sensing of formaldehyde as well as photocatalytic degradation of dyes are checked.

1.8 Objective of the Study

1.8.1 General Objective

- Synthesis of the nanomaterial for the sensing of heavy metals and application in sensing of formaldehyde as well as photocatalytic degradation of dyes.

1.8.2 Specific Objectives

- Preparation of the extract of rhizome of *Curcuma longa.*
- To synthesize the AgNPs using an aqueous extract of the rhizome of *Curcuma longa.*
- To study the stability and size of the AgNPs using UV spectroscopy, X-ray diffraction.
- To study the metal sensing activity of synthesized AgNPs.
- To study the photocatalytic degradation of dyes
- To study the sensing of Formaldehyde.

CHAPTER II

2 LITERATURE REVIEW

2.1 Plant Description

Turmeric (*Curcuma longa*) is a flowering plant of the ginger family with a long history of medicinal use due to its potent anti-inflammatory properties. Its most active constituent is curcumin, which has been widely studied. However, curcumin has extremely limited bioavailability (Wen et al., 2007). A tall herb with broad, oblong leaves that are pale green on the underside and dark green on the upper surface. It's little, brown seeds are found in the yellow-white flowers that grow on a spike-like stalk. The only means of reproduction for turmeric is through its strong underground stem, or rhizome, which is surrounded by the roots of previous leaves.

Classification of Plant

Kingdom: Plantae

Phylum: Tracheophyta

Class: Liliopsida

Order: Zingiberales

Family: Zingiberaceae

Genus: *Curcuma*

Species: *longa*

Figure 2.1: *Curcuma longa*

The rhizomes are finger-like lateral offshoots that branch out from a central bulbous part and are brownish-yellow in hue. The rhizome contains a significant amount of the distinctive yellow substance, even though it is present throughout the entire plant. Turmeric comes in many kinds that can be identified by the names of the places where they are grown. It is believed that turmeric grown in the hills is of higher quality than turmeric grown on the plains. The quality and yield of even the same variety planted in the plains and on the hills differ significantly (Kovatcheva, n.d.). The tuber of this plant

is of great medicinal value. The juice of the fresh rhizome is used as an anti-parasitic for many skin diseases. Oil of turmeric, distilled from the dried rhizome, shows antiseptic properties.

2.2 History of Nanomaterials

For more than 2,000 years, colloidal silver and gold have been used medicinally and have been crucial to preserving human health. To maintain a healthy immune system, ancient Greece, Egypt, Macedonia, and Rome employed silver. The "father of medicine," Hippocrates, noted in his medical writings that silver possessed advantageous curative and disease-preventive powers. He lauded silver for its capacity to heal wounds and regenerate tissue (Daniel & Astruc, 2004).

The word "Nano" is derived from the Greek word, which means "dwarf" (Rai et al., 2008) Richard Feynman introduced the idea of nanotechnology on December 29, 1959, at a speech at the California Institute of Technology (Feynman, n.d.). Also, Norio Taniguchi first used the word "Nanotechnology" in 1974 to describe one molecule's ability to process, distort, and consolidate material (Corbett et al., 2000). The same bulk material has different characteristics at the nanoscale. Metal nanoparticles are employed in a wide range of applications, including bio composite production, the production of electronic devices, the healing of wounds, and anti-bacterial properties (Ramsden & Tóth-Boconádi, 1990).

Several physical and chemical methods, including milling and chemical degradation, were used to mediates nanoparticles and increase their effectiveness at the beginning of the 20^{th} century (Ahmad, et al., 2016a). However, these traditional methods use expensive and hazardous chemicals and cannot be regarded as an environmentally friendly procedure of nanoparticles (Vijayan et al., 2016). nanoparticles .The manufacture of metal and metal oxide NPs using a bio-genic process, which involved aqueous plant extract and bacteria, has recently attracted the attention of finders because it is stable, clinically adaptable, biocompatible, and cost-effective (Ahmad, et al., 2016a), (Annu, et al., 2016). Utilizing plant extract, microbes, and other materials, several metal and metal oxide nanoparticles have already been produced (Olteanu et al., 2016). Plant biomass is extensively sought after by our organization and others as a catalyst for chemical methods in addition to its extensive uses in the production of NPs due to its global availability, renewability, and environmentally friendly character

(Changmai et al., 2019; Rajkumari et al., 2019) and biodiesel productions (Changmai et al., 2020; Nath et al., 2019).

Because of the simplicity of their manufacture and chemical changes, AgNPs are special in nanoscale systems. AgNPs are utilized in the creation of novel technologies in the fields of electronics, material sciences, and medicine. As a result of their wide range of applications, experts from all over the world are conducting more studies on AgNPs (Mulvaney, 1996). A rare combination of valuable properties, including high electrical double-layer capacitance, catalytic activity, well-developed surfaces, and unique optical properties associated with the Surface Plasmon Resonance (SPR), is displayed by silver nanoparticles, according to fundamental studies conducted in the last three decades (Meyers et al., 2006). Because of this, these are used as a material in the creation of novel electrical, optical, and sensor devices.

Researchers have focused a lot of their emphasis recently on developing efficient green chemistry methods that produce silver nanoparticles with the required morphology and size by employing natural reducing, capping, and stabilizing compounds. AgNPs can be produced using biological techniques rather than harsh, hazardous, or expensive chemical agents (Ankamwar et al., 2005; Bhainsa & D'Souza, 2006). Considering green synthesis, compounds with dual properties, such as reducing and capping agents, are favored nowadays since the reaction only requires one step (Mohanpuria et al., 2008).

Several fungi species were used to mediate the formation of nanoparticles of various sizes including Aspergillus niger (Janardhanan et al., 2013), *Neurospora crassa* (Castro-Longoria et al., 2011), *Fusarium solani* (Šebesta et al., 2023), etc. The first time generated of AgNPs was reported using the bacteria *Pseudomonas stutzeri* AG259 strain (Haefeli et al., 1984). Other reports that demonstrated the use of other bacterial strains in the synthesis of AgNPs are; *Escherichia coli* (El-Shanshoury et al., 2011), *Bacillus subtilis* (Saifuddin et al., NaN/NaN/NaN),etc. Similarly, extracellular mediated of AgNPs by several algal species has been reported. The marine alga such as; *Chaetomorpha linum* (Kannan et al., 2013), *Caulerpa resmosa* (Kathiraven et al., 2015)and *Sargassum polycystum* were also explored to synthesize AgNPs.

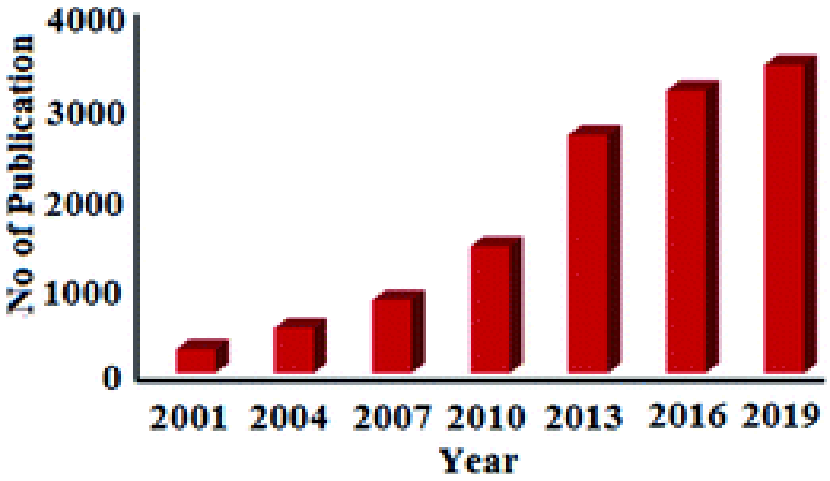

Figure 2.2: Yearly publications on green silver nanoparticle production from 2001 to 2019

(Vanlalveni et al., 2021)

The statistical data analysis in Fig. 1 showed an increase in the number of research publications that have been published in the field of biogenic synthesis of AgNPs. The term "Green synthesis of silver nanoparticles" was used in the "SciFinder Database" to find these data in September 2020. It has grown dramatically from a meager 259 publications in 2001 to 3374 publications in 2019. Thus, the goal of this review is to encourage researchers to investigate natural resources for the production of silver nanoparticles using a variety of plants and their organs, a process known as nanobiotechnology. This review will also provide strategies for using several routes to produce silver nanoparticles that can benefit people.

Azadirachta indica (neem) leaves served as an inspiration for the synthesis of AgNPs, according to Verma and colleagues, who also assessed how the pH of the solution affected the growth of nanoparticles (Verma & Mehata, 2016). By altering the charge of the biomolecules, which may affect both their capping and stabilizing capabilities, a change in pH has an effect on the shape and size of the particles. They have observed that the UV spectrum's absorption maxima moves from 383 to 415 nm as the pH climbs from 9 to 13, indicating an increase in absorption intensity. Anandalakshmi and coworkers showed that Pedalium murex leaf extract produced AgNPs (Anandalakshmi et al., 2016). When tested against a range of bacteria, the produced NPs displayed the highest ZOI of 10.5 mm (on a 15 L mL1 scale) against E. coli and P. aeruginosa and the lowest activity against Klebsiella pneumoniae (8.5 mm). The size and shape of the resultant AgNPs were clarified using TEM. The particles had diameters of about 50 nm

and were primarily spherical, according to the TEM images. Ahmed et al. reported Azadirachta indica increased AgNP production (Ahmed et al., 2016).

In contrast to the plant extract, the generated NPs showed equivalent potency (9 mm ZOI) against *E. coli* and *S. aureus*. More recently, AgNPs with an average size of 3.46 nm were made utilizing a leaf extract from the *Solanum nigrum* plant (Vanlalveni et al., 2021)

With NPs as tiny as 1.74 nm, this is one of the tiniest biogenic AgNPs ever documented. AgNP production was verified by SPR bands in UV-visible spectroscopy at 442 nm. The effectiveness of AgNPs as an antibacterial agent is strongly influenced by the shape of the nanoparticles, according to several cited literature. When circular, disc-like, and triangle-shaped AgNPs were compared to each other as antimicrobial agents, spherical AgNPs were shown to be more active than disc-like AgNPs and triangular AgNPs (Madivoli et al., 2020), (Lee et al., 2016). *Coptis chinensis* rhizome extract was used for the green synthesis of AgNPs with a size of 15 nm. Chitosan was used to make additional surface modifications to the synthesized AgNPs. AgNPs, both unmodified and chitosan-modified, were examined for their bactericidal ability against B. subtilis and E. coli bacteria. According to the findings, the chitosan-modified AgNPs were more effective at inhibiting the bacterial strains than free AgNPs. Recently, rhizome extract of *Coptidis* (Khan et al., 2019), *Curcuma longa* (turmeric), (Alsammarraie et al., 2018), *Canna indica* L. (Selvi et al., 2019)and *Ferula foetida* (asafoetida gum) (Devanesan et al., 2020) was used for the green synthesis of circular AgNPs with size in the nanometer range. Several bacterial strains were used to test the generated AgNPs for their bactericidal activity, and it was shown that the NPs are effective at causing bacterial cell destruction. The AgNPs produced by Canna indica L. shown superior bactericidal activities against E. coli when compared to other bacteria including S. aureus and K. pneumoniae. However, while comparing the bactericidal activity of Canna indica L. produced AgNPs with that of Gentamicin, it was found that the NP is less effective than Gentamicin (Vanlalveni et al., 2021).

Table 2.1: Various rhizomes extract used for the green synthesis of AgNPs

S.N	Plants	Plant parts	Shape and size	References
1	*Bergenia ciliate*	Rhizome	Spherical; 35 nm	(Phull et al., 2016)
2	*Dryopteris crassirhizoma*	Rhizome	Spherical; 5–60 nm	(Lee et al., 2016)
3	*Coptis chinensis*	Rhizome	Spherical; 15 nm	(Lok et al., 2006)
4	*Coptidis rhizome*	Rhizome	Spherical; 30 nm	(Sharma et al., 2018)
5	*Curcuma longa (T*urmeric)	Rhizome	Spherical; 18 ± 0.5 nm	(Alsammarraie et al., 2018)
6	*Canna indica* L	Rhizome	Spherical; 20–70 nm	(Selvi et al., 2019)
7	*Ferula foetida* (asafoetida gum)	Rhizome	Spherical; 5.6–8.6 nm	(Devanesan et al., 2020)

(Vanlalveni et al., 2021).

When the produced AgNPs were used to test their antibacterial efficacy against different kinds of bacteria, it was found that they have good cell disruption capabilities. The research reported a quick, easy approach for making environmentally friendly C-Ag nanoparticles and suggests its multidimensional nano application in the pharmaceutical, medicinal, and food refining industries. That work also showed that by adjusting the weight of curcumin, which was utilized as a reducing and capping agent in the reduction process, the size and quality of C-Ag NPs could be improved (Khan et al., 2019a). Curcumin (CUR), a natural polyphenol derived from turmeric with documented antibacterial, antioxidant, and anti-inflammatory activities, is a well-known remedy for healing wounds (Gupta et al., 2019). Along with its medicinal properties, CUR has been used to produce AgNPs as a reducing and capping agent (Gupta et al., 2020).

Numerous studies have recently been undertaken on the effects of curcumin or curcumin nanoparticles alone or in conjunction with other food additives on monogastric farm animals, poultry, and fish. This work also showed that by adjusting the weight of curcumin, which is utilized as a reducing and capping agent in the reduction process, the size and quality of C-Ag NPs could be improved. However, in-vitro investigations and edible polysaccharide films have not yet taken use of the antibacterial and antimicrobial capabilities of these green-produced C-Ag NPs (Khan et al., 2019b). Silver nanoparticles have gained popularity recently for the treatment of

wounds. In the present study, Curcumin, a naturally occurring polyphenolic compound, which is popularly utilized as a wound-healing agent, was used as a natural reducing agent to produce green nanoparticles (Gupta et al., 2020). Since biosynthesis of Ag-NPs utilizing green resources like *C. longa* is pollution- and environment-free, it is preferable to chemical synthesis. One can conclude from the findings of this study that C. longa tuber powder can be useful in the bio-reduction and stabilization of silver ions to Ag-NPs (Shameli et al., 2012). These nanoparticles made from turmeric oil have the potential to function well as antioxidants. As a result, it can be utilized for mass production and the targeted administration of medications for conditions such as cancer, dermatitis, AIDS, and excessive cholesterol (Christopher et al., 2021).

Environment and human health may be negatively impacted by heavy metal ions, it is crucial to monitor the concentrations of potentially harmful metal ions in aquatic ecosystems (Campbell et al., 2003). Copper in drinking water at high levels is harmful to human health, and it is extremely hazardous to many bacteria and viruses as well as algae, (Alvarez et al., 2021). According to Zietz and his coworker, several occurrences of liver injury in infants have been linked to high copper intake (Zietz et al., 2003). Due to the high toxicity of many Hg compounds or mercury-based pollutants, which are mostly produced by coal-burning power plants, are a major environmental issue (Wang et al., 2004). Hg^{+2}, one of the most dangerous metal ions, damages a number of human body parts causing severe symptoms and declining health (Zahir et al., 2005; Zheng et al., 2003). To safeguard the environment and the general public's health, it is crucial to develop sensitive and focused methods for detecting the presence of Hg^{+2} and Cu^{+2} ions.

Cu^{+2} and Hg^{+2} ion detection techniques have been widely documented up to this point. The majority of them include chromogenic sensors (Banthia & Samanta, 2005), chemosensors with chemodosimeter (Kim et al., 2008), functionality fluorescent chemosensors (Zhang et al., 2011) inductively coupled plasma mass spectroscopy (Becker et al., 2007) and ICP-AES (Inductively Coupled Plasma Atomic Emission Spectroscopy) (Liu et al., 2005) for detection of Cu^{+2} ions. . Thin gold films (Morris & Szulczewski, 2002), polymeric materials (Tang et al., 2006), bio-composites (Ono and Togashi 2004), chemosensors (Lee et al., 2009), and other materials can be used to create chemical sensors for the detection of Hg^{+2}.

It is still conceivable to create new, practical assays to find Cu^{+2} and Hg^{+2} in real samples. The exploration of colorimetry using gold and silver nanoparticles for chemical detection and biosensing of various substances (Zhao et al., 2008), including viruses (Niikura et al., 2009) a malignant cell (Medley et al., 2008), toxins (Uzawa et al., 2008), heavy metals (Fan et al., 2009; Mulyaningsih et al., 2023), pesticides (Barman et al., 2013), and numerous more organic and inorganic contaminants in water have increased recently (Daniel et al., 2009; Xiao & Yu, 2010).

It is well known that AgNPs and their composites display higher catalytic activity in the area of dye degradation and removal. Kundu and coworkers studied the methylene blue degradation by arsine in the presence of silver nanoparticles (Ghosh et al., 2002). The reduction of the phenosafranine dye was also examined by Mallick and coworkers using the catalytic activity of these nanoparticles (Mallick et al., 2006).

2.3 Research Gap

Most researches have been carried out by chemical method for the synthesis of silver nanoparticles but few researches are known on the green synthesis method. Silver nanoparticles are used comparatively less in degradation of harmful organic dyes. Considering the growing threats to all living organisms, researchers have drawn attention in the metal sensing activity using nanoparticles as their identification is the most. This present research emphasizes the green synthesis of silver nanoparticles which is still very challenging because only a few works have been done. Besides that, this work also focuses on its application in organic dyes degradation and metal sensing activity.

CHAPTER III

3 MATERIALS AND METHODS

The present study was performed at the Laboratory of the Central Department of Chemistry, Tribhuvan University, Kritipur. The details of materials, experiments, and procedures employed throughout this research were discussed as follows:

3.1 Materials

3.1.1 Chemicals

The following chemical reagents were used in this research: $AgNO_3$ (Fischer Scientific), distilled water, Ethanol, Whatman Filter Paper No. 1, NaOH, $CrCl_3$ (Himedia), $ZnSO_4.7H_2O$ (E. Merk), As_2O_3, $HgCl_2$ (Fischer Scientific), $BaCl_2.2H_2O$ (Analar), $Ni(NO_3)_2.6H_2O$ (Merk), $CuCl_2.2H_2O$ (Fischer Scientific), $MnSO_4$ (Fischer Scientific), $NaBH_4$,. All the chemicals and materials were used as provided by the company without any further purification.

3.1.2 Plant Material

The plant material used in this study was *Curcuma longa.*

Figure 3.1 : Powder of *Curcuma longa* rhizome (Li et al., 2020)

Figure 3.1 is the figure of powder of *Curcuma longa* rhizome. *Curcuma longa* commonly known as "Besaar" belongs to Zingiberaceae family, genus *Curcuma.* It is a tropical climate-adapted tuberous herbaceous perennial plant with yellow flowers and broad leaves (Akpolat et al., 2018; Prasad et al., 2014). Coughs, diabetes, dermatological ailments, respiratory issues, cardiovascular and hepatobiliary diseases, arthritis, irritable bowel syndrome (IBS), peptic ulcers, psoriasis, and atherosclerosis are just a few of the illnesses for which the turmeric plant is utilized as a traditional medication and treatment (Kenawy et al., 2019). Turmeric plants typically contain 0.76% alkaloid, 0.45% saponin, 0.03% sterol, 0.82% phytic acid, 0.40% flavonoid and 0.08% phenol. Fresh tuber of *Curcuma longa* was collected from the hometown Tilottama-2, Rupandehi. The air-dried tuber of the plant was used for the experimental work.

3.2 Biosynthesis of AgNPs

The biosynthesis of AgNPs using *Curcuma longa* extract was done by following a reported procedure with some modification (Chandraker et al., 2019).

3.2.1 Preparation of Plant Extract

The harvested tuber was properly cleaned with running tap water and then with distilled water. It was then left to dry at room temperature for fifteen days in the shade. An electrical blender was used to turn the air-dried tuber into powder, which was then stored in plastic bags for future use. 2 g of the powder sample and 100 mL of distilled water were heated at 40 ℃ for around 30 minutes on a magnetic stirrer to create the tuber broth solution. They were first filtered through regular filter paper and then Whatman Filter Paper No. 1 after cooling at ambient temperature. The residual extract was retained at 4 °C for future studies, while the filtrates from the filtration process were employed for the tests.

3.2.2 Preparation of Silver Nitrate Solution.

A volumetric flask was used to combine 4.247g of $AgNO_3$ with 500 mL of distilled water to create a stock solution that contains 50 mM $AgNO_3$. 1mM $AgNO_3$ was prepared by diluting 10 mL of the stock solution to 500 mL in order to create AgNPs. For next tests, all of the solutions in volumetric flasks were covered in a black covering and kept in the dark.

3.2.3 Biosynthesis of AgNPs

For the reduction of Ag^{+} ions, 5 mL of plant extract was mixed dropwise to 20 mL aq. $AgNO_3$ solution on a stirrer for 35 minutes at 25°C and kept for 24 hr at dark for further analysis. The solution's pH was stabilized at 11 by mixing 0.1 M NaOH. It was noticed that the solution colour has changed. To verify a formation of AgNPs, the UV-Vis spectra were taken at various time intervals.

3.2.4 Purification of AgNPs

The solution was centrifuged using a Sorvall ST 8R centrifuge at 8500 rpm for 25 minutes at room temperature after being reduced for 24 hours. The resulting particle was disappeared in distilled water after the supernatant liquid was removed. For the removal of any substance that had been adsorbed to the plane of the AgNps, the centrifugation operation was repeated three times. Absolute ethanol was then added. As a result, for further investigation, pure AgNPs were preserved in a dessicator which was kept in an eppendorf tube and fully covered with aluminum foil.

3.3 Characterization Techniques

X-ray Diffraction (XRD), Fourier Transform Infra-Red (FTIR), and UV-Vis spectrophotometers were used to characterize the synthesized AgNPs**.**

3.3.1 UV-Vis Spectroscopy

The optical property of AgNPs was decided by UV-Vis spectrophotometer (Specord,Germa 200 plus, Germany). After $AgNO_3$ was added to the solution of plant extract, the spectra were observed in various time intervals between 300 nm to 700 nm. The UV-Vis spectra were taken by diluting (10 times) the nanoparticle dispersion. To examine the stability of the nanoparticle, UV-Vis spectrum was taken up to 1 month.

3.3.2 Fourier Transform Infra-Red (FTIR)

An FTIR spectrometer (Perkin-Elmer LS-55-Luminescence spectrometer) was used to determine the chemical makeup of the produced AgNPs. The dried powders were characterized from the range 4000–500 cm^{-1}.

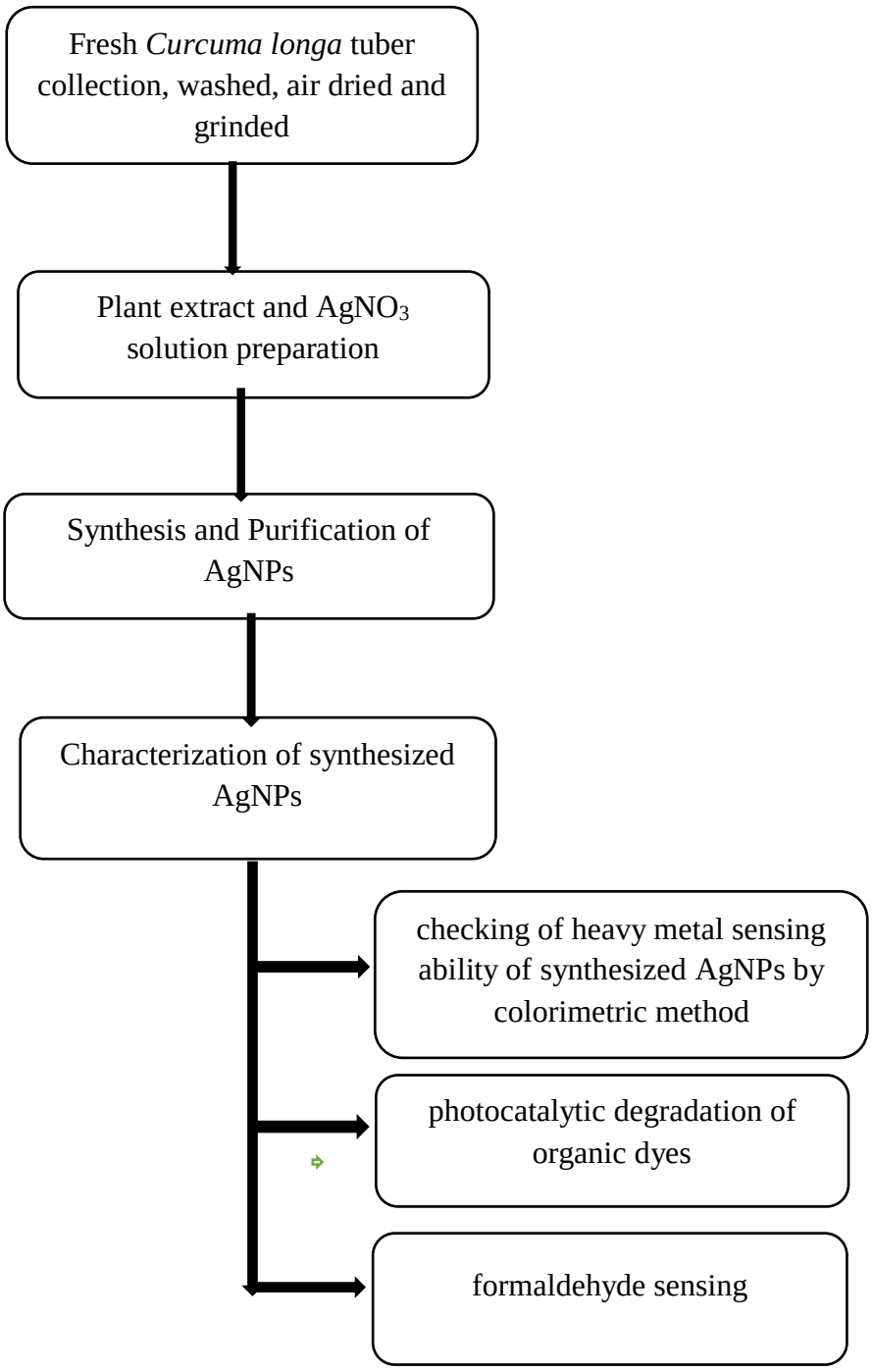

Figure 3.2: Schematic representation of various steps involved in the execution of experiments

3.3.3 X-ray Diffraction (XRD)

By using X-ray diffraction spectroscopy (Philips PAN analytical) in NAST, it was possible to detect the different phases and grain sizes of synthesized AgNPs. With CuKα radiation, the produced AgNPs were examined at 30 kV of voltage, 20 µA of current, and 0.030/s of scan speed. The phases that were present in the synthesized

samples were determined utilizing the search and match feature of the X′pert high score software. Normally, the working environment were typically 2 theta scanning temperature from 20 to 90 degrees. The particle size of the obtained samples was calculated by using Scherer's equation as follows:

$$D = \frac{K \times \lambda}{\beta \, Cos\theta}$$

Where, D = crystallite or grain size,

K= Dimensionless shape factor, of a value close to unity (~0.9)

λ = Wavelength of the radiation, (0.154 nm for Cu Kα)

θ = Bragg's angle (the 2θ value of chosen peak) in radian

β = Full width at half maximum of the XRD peak (should be in radian)

3.4 Metal Sensing Activity of AgNPs

The metal sensing activity of the synthesized AgNPs was performed by the colorimetric method with some modifications (Puente et al., 2019).

3.4.1 Preparation of Metal Salt Solution

The solution of the 10 different heavy metal salts was prepared in deionized water. For the preliminary test, 0.01M solution of each metal salt was prepared.

The amount of salt required to prepare the solution was calculated by using the formula:

$$\text{Weight taken} = \frac{\text{Molarity (0.01M)} \times \text{Molecular weight (grams)} \times \text{Volume (mL)}}{1000}$$

For the further experiment, the solution was diluted by adding distilled in the required volume.

Table 3.1: The amount of metal salt required for the experiment

Salt Used	Molecular Weight (in grams)	Weight(W)
$CrCl_3.6H_2O$	266.45	0.266
$ZnSO_4.7H_2O$	287.54	0.288
$HgCl_2$	271.50	0.272
As_2O_3	197.84	0.198
$BaCl_2.2H_2O$	244.21	0.244
$Ni(NO)_3.6H_2O$	290.81	0.291
$CuCl_2.2H_2O$	170.48	0.170
$MnSO_4$	169.06	0.169

W= Weight required to prepare 0.01 M in 100 mL (in grams)

3.4.2 Metal Colorimetric Sensing

In a standard detection test, 4 mL of a noble metal nanoparticle dissolution were combined with 1 mL of the metal solution. The ions that were used for the experiments were , Ba^{2+}, Hg^{2+}, Cu^{2+}, Mn^{2+}, Zn^{2+}, As^{3+}, Ni^{2+}, and Cr^{3+}at a concentration of 0.01M. UV-Vis spectrophotometry was used to observe and assess the color change of the resultant solution.

By reducing their concentration, metal ions sensed during the first phase of the experiment were further examined.

In order to evaluate the detection limit of the produced AgNPs, different volumes (20–600 µL) of that metal ion were blended with 1 mL of the nanoparticle dissolution. After that, UV-Vis spectrophotometry was used to analyze the resulting dispersion.

3.5 Dye Degradation Assay

AgNPs have the peculiar potential of degrading organic dye therefore they can be applied in various organic dyes such as methylene blue (MB) and Methyl orange (MO). This research was mainly focused on the activity of methylene blue and Methyl orange using AgNPs with the aid of hydrogen peroxide (H_2O_2).

In the beginning, the stock solution of methylene blue and methyl orange was prepared to dissolve 25 mg of MB and MO in 250 mL of distilled water for the 1000 ppm concentration and again it was diluted to 100 ppm concentration. Then 2 mL of AgNPs with 2 times dilution was mixed to 20 mL of dye solution in the presence of 0.5 Mor % H_2O_2 following the continuous exposure to sunlight. Then, a color shift was noticed while being periodically examined by a UV-Vis spectrophotometer at precise time intervals. At various time intervals, the absorbance maxima were measured in order to track the reactivity of the resultant solution. The degradation efficiency was estimated as:

$$Efficiency\ (\%) = \frac{Ao - A}{Ao} * 100$$

In which, efficiency (%) represents the degradation efficiency of dye

A_O=absorbance of dye solution at zero time

A= absorbance of dye solution in suspension after time t

3.6 Detection of Formaldehyde Solution

For this experiment, in the inception, 40% formaldehyde solution was taken and diluted in the various concentration such as 30%, 20%, 10%, and finally 1% then in each test tube 2 mL of each concentration was taken and 1 mL of silver nanoparticle with dilution was added to each of them then alteration color of the resulting solution was discerned and all of them were monitored using the UV-Vis spectrophotometer for the further confirmation.

3.7 Data Analysis

Data analysis and graphical plots were performed using X' pert high score plus, Image J, Origin 2019b, and MS Excel.

CHAPTER IV

4 RESULTS AND DISCUSSION

4.1 Green synthesis of AgNPs

The green synthesis of AgNPs was followed by a distinct color change. The aqueous $AgNO_3$ solution and turmeric extracts were initially colored yellow (Figure 4.1). However, the mixture's hue evolved from light brown to brown to brown-reddish after 24 hours of gently stirring at room temperature. This shift in color was seen as confirmation that the AgNPs had been successfully synthesized. The aqueous solution's color shift may be caused by the surface excitation of the plasmon resonance phenomenon of silver metal (Shameli et al., 2014). Turmeric powders contain some proteins as well as terpenoids. Additionally, turmeric includes higher levels of compounds including sesquiterpenes, zingiberene, and -phellandrene (Sathishkumar et al., 2010). Curcumin, a polyphenolic bioactive ingredient that greatly contributes to its distinctive flavor and color, makes up the majority of these components

After adding plant extract and $AgNO_3$ Colour changed after 24 hr

Figure 4.1: Colour change during the synthesis of AgNPs nanoparticles

. According to studies, proteins found in turmeric powder served as capping agents for the AgNPs, preventing them from aggregating in AETP and helping to stabilize the biosynthesized AgNPs. These substances are cysteine or residues of free amino groups

(Gole et al., 2001). Sathishkumar and coworkers proposed a method for stabilizing AgNPs that uses proteins extracted from the *C. longa* tuber powder as a capping agent (Sathishkumar et al., 2010). Strong reducing agents, these functional groups led to the production of metal nanoparticles (Asti et al., 2014; Sankar et al., 2017; Zhao et al., 2010).

4.2 Characterization of AgNPs

4.2.1 UV-Vis Spectrometry

The resulting nanoparticles' size, shape, morphology, composition, and dielectric environment change the SPR bands (Kelly et al., 2003; Stepanov, 2004). It is obvious from UV-visible absorption spectra (figure) that the broad SPR band had a peak at 426 nm after 24 hours of stirring. This peak demonstrates the presence of a constant dispersion of hydrosol silver nanoparticles (Loiseau et al., 2019; Zargar et al., 2011). The sample's absorption spectra were evaluated for the Ag-NPs emulsion stability test after 48 hours and even after 20 days (figure 4.2). The spectra for these two samples indicated slight changes in their peak strength, although that the Ag-NPs absorption peak changed slightly from 426 to 427 nm. The absorption peak of 48 hr and 20 days are the same, which is almost the same as the absorption peak recorded at 24 hr of synthesis. It was also reported that initial visual confirmation of the color change from pale white to reddish brown and subsequent confirmation of the production of AgNPs by UV-visible spectra taken at various times provided preliminary evidence. AgNPs are confirmed by a sharp peak in the UV-visible spectrum at an absorption wavelength between 400 and 450 nm (Singh et al., 2014). The absorption peak of this nanoparticle is almost the same as the reported in article which confirms the presence of AgNPs.

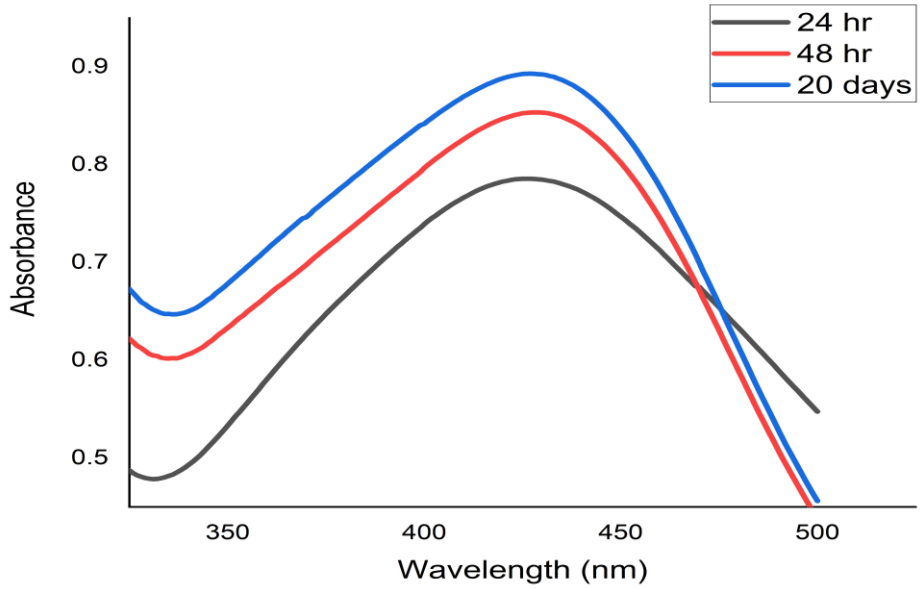

Figure 4.2 : UV-visible absorption spectra of *Curcuma longa* at different time 24 hr, 48 hr and 20 days.

4.2.2: X-Ray Diffraction

XRD was used to determine the crystallite or grain size of the synthesized AgNPs. The distinctive peak exhibited in the XRD image further displayed and demonstrated AgNPs made with *Curcuma longa* extract (Figure 4.3).

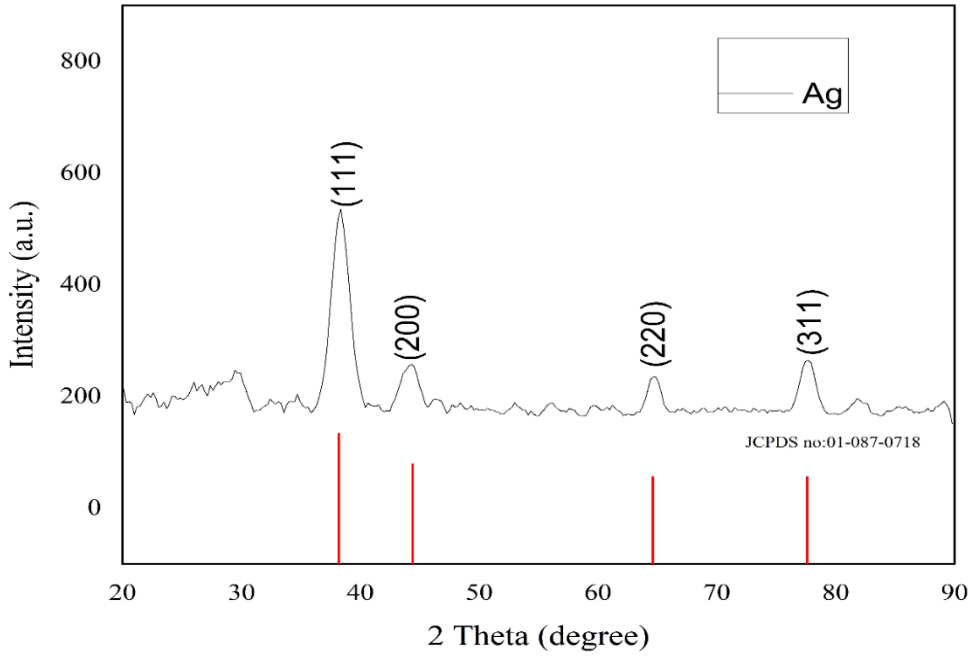

Figure 4.3: XRD patterns of *Curcuma longa* mediated AgNPs

The four distinct diffraction peaks of the 2 theta values of 38.32^0, 44.16^0, 64.70^0 and 77.64^0 can be, accordingly, indexed as (111), (200), (220), and (311). The typical face center cubic (FCC) silver lines that connect all diffraction peaks are in greater accord with the powder data of JCPDS file no 01-087-0718. The XRD pattern makes it abundantly evident that the AgNPs made using *Curcuma longa* are crystalline.

Table 4.1: Calculation of size of IONPs

No.	2θ (in degree)	h k l	FWHM	Grain size (nm)	Average grain size (nm)
1	38.32	1 1 1	1.745	5.033	6.66
2	44.16	2 0 0	1.521	5.883	
3	64.70	2 2 0	1.193	8.230	
4	77.64	3 1 1	1.418	7.509	

Using the Debye-Scherrer formula, the average crystallite size of AgNPs was calculated from the FWHM of peaks and was found to be 6.66 nm. The identical outcome, which demonstrates that the AgNPs are crystalline in nature, face-centered, and cubic, as reported by Roy and coworkers (Roy et al., 2015).

4.2.3 Study of Biomolecular Reduction by FTIR

To learn more about the functional groups that are active in the biomolecules involved in the bioreduction of Ag^+ and the capping of AgNPs, FTIR spectra of both *Curcuma longa* extract and synthetic AgNPs were conducted. The range that the FTIR analysis has shown is 500 to 4000 cm^{-1}.

The FTIR spectra indicate the absorption bands at 3262, 2929, 2848, 1632, 1518, 1435, 1373, 1219, and 1045 cm^{-1} showed the presence of capping agents with the nanoparticles as shown in Figure 4.4 (A).

The broad and strong band at 3262 cm^{-1} was attributed to the O-H stretching vibration of alcohol and phenol. The bands at 2929 cm^{-1} and 2848 cm^{-1} correspond to the aromatic compound C-H stretching vibration. The presence of C-C and C-N stretching

vibrations, which caused the peaks at 1632 cm^{-1}, indicated the existence of proteins (Prakash et al., 2013). N-H stretching vibrations, which are found in the amide linkage of the proteins, reached their peak at 1435 cm^{-1}. The proteins' N-H and C-N (amines) stretch vibrations were assigned to the bands at 1373 cm^{-1} and 1045 cm^{-1}, respectively. The elongation of the C-N bond in amines led to the band at 1219 cm^{-1}. The weak broad strong signal at 3262 cm^{-1} in nanoparticles shows that the extract's -OH group was engaged in the reduction of silver ions. Since the peak at 1045 cm^{-1} can be attributed to the C-OH of the phenols, which support the reduction of Ag^{+} into Ag° by the sharing of polyphenols like flavanoids and triterpenoids, these results are more in line with Litvin and Minaev's findings (Litvin & Minaev, 2013).

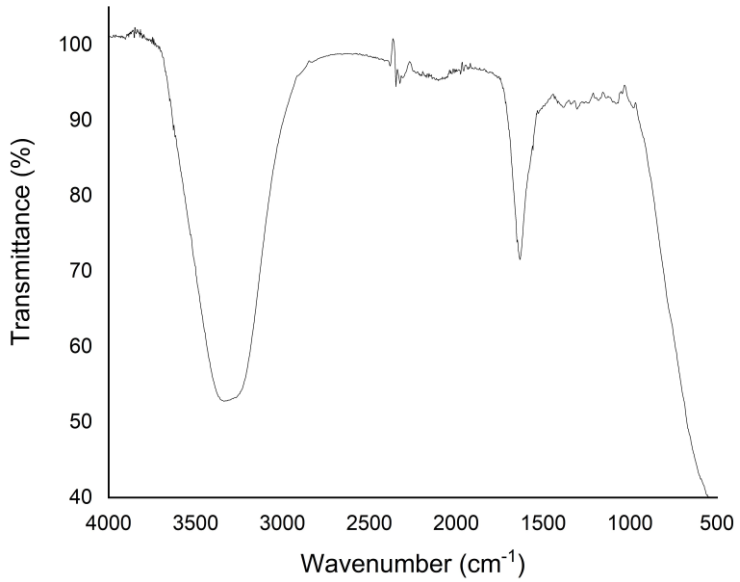

(A)

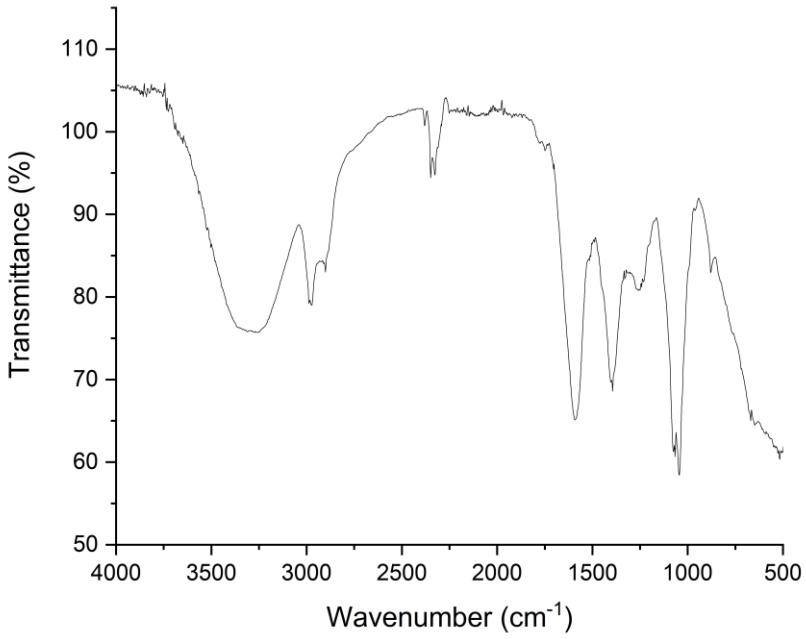

(B)

Figure 4.4: FTIR spectra of: **(A)** *Curcuma longa* extract **(B)** AgNPs

4.3 Application of Synthesized AgNPs in Analysis

Using plant extract to synthesis AgNPs is a quick, efficient, and environmentally friendly method that was applied in this study. AgNPs may have numerous analytical uses in various industries. In this work, some of them were investigated.

4.3.1 Colorimetric Sensing of AgNPs

AgNPs mediated by *Curcuma longa* were used to investigate the selective colorimetric sensing capability for several heavy metals in an aqueous solution. For the colorimetric detection in this work, 8 different metal ions were tested.

The color change of AgNPs following the addition of several heavy metal solutions with a concentration of 0.01M can be seen in the figure 4.5.

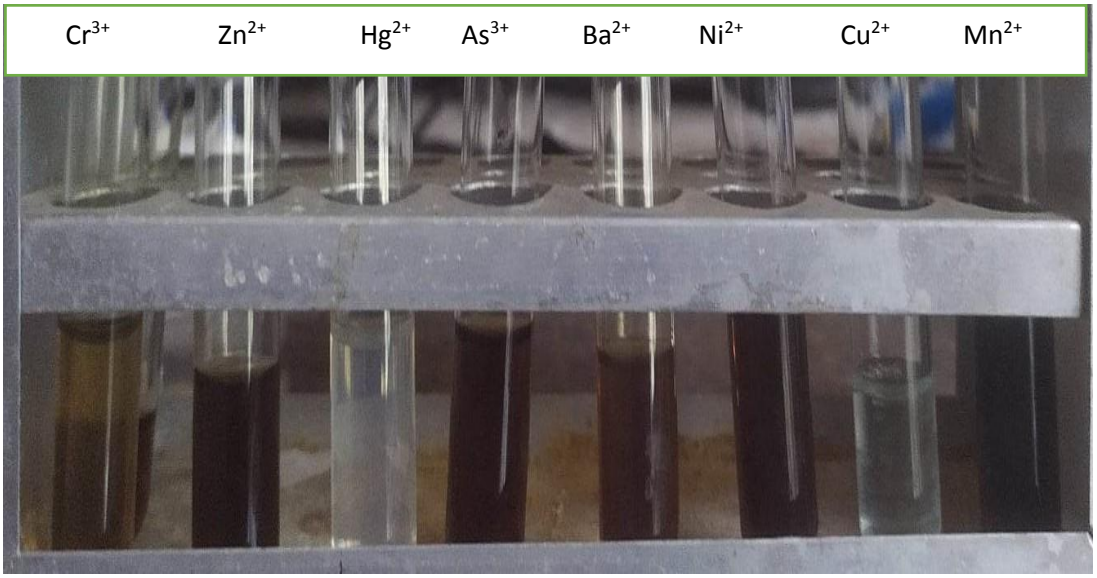

Figure 4.5: Color change of nanoparticle dispersion after the addition of the metal solution

After the addition of 0.01M metal solution, max value underwent a bathochromic shift, and the AgNPs' absorbance decreased, with the exception of Hg^{2+}, as shown in (figure. 4.5).

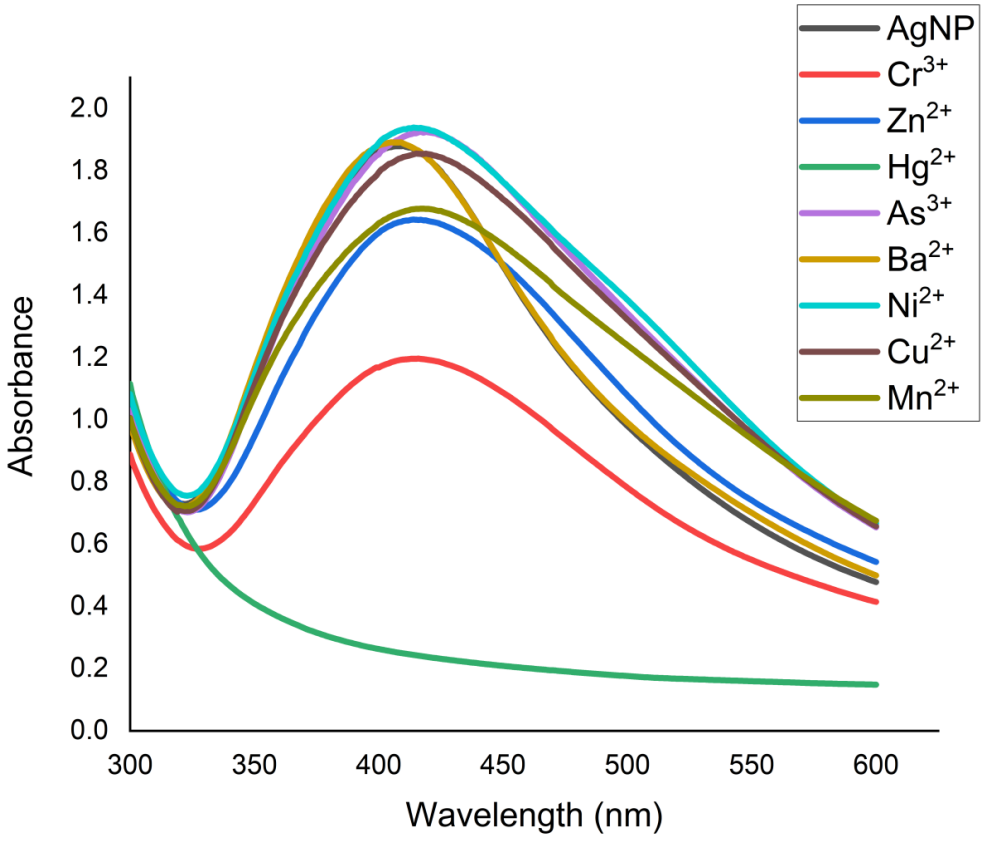

Figure 4.6: UV-Vis spectra of Silver NPs dissolution with various metal ions.

While no noticeable color change was seen in the remaining metal solution, the reddish brown colored AgNPs solution was selectively transformed by the addition of Hg^{2+} into a completely colorless solution that is readily visible to the naked eye.

The λ_{max} value of AgNPs did not change significantly when Cu^{2+} was added (418 nm to 417 nm); nevertheless, Fe^{2+} showed the greatest shift (417 nm to 435 nm). Ni^{2+} and Zn^{2+} ions showed a comparable red shift in the SPR absorption of AgNPs from 418 nm to 430 nm. The max value of AgNPs shifted from 417 nm to 425 nm, 423 nm, 428 nm, 421 nm, and 429 nm when further metal ions Ba^{2+}, Cr^{3+}, Mn^{2+}, As^{3+}, and Cd^{2+} were introduced.

AgNPs and Hg^{2+} failed to show a peak in their dispersion, which may have been the result of Hg^{2+} interacting with the biomolecules that had been adsorbed on the surface of the AgNPs. The newly created biologically formed AgNPs had a significant SPR absorption band and were yellowish-brown in color. The silver NPs solution which was previously yellow became uncoloured in the presence of Hg^{2+}, and the SPR band expanded and shifted to blue. This shows that AgNPs have a specific sensitivity to the Hg^{2+} ion.

4.3.1.1 Sensitivity of AgNPs towards Hg^{2+} Ions

By adding various volumes of Hg^{2+} ions mixture to the 1 mL AgNPs dissolution at 25 °C, the sensitive nature of the green-produced AgNPs was investigated. A noticeable color change and UV-Vis spectra were used to determine the smallest detectable Hg^{2+} ion in the aqueous system. The figure shows the color shift that occurred after mixing the various volumes of Hg^{2+} mixtures sequentially from 20 to 600 µL. From yellowish brown, yellow, light yellow, and translucent salmon, the color shifted to transparent.

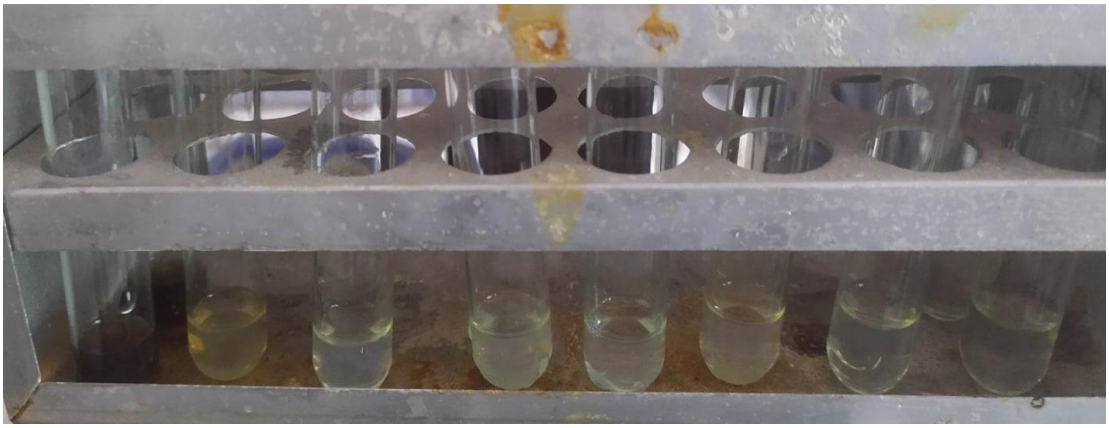

(A)

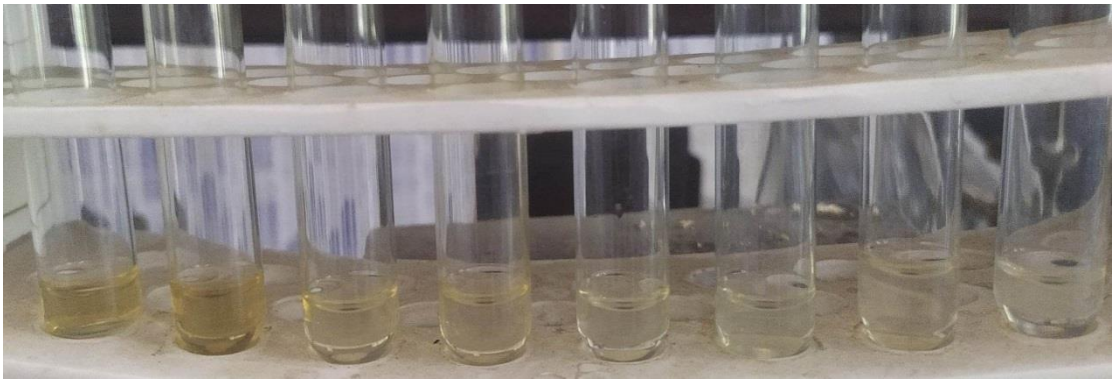

(B)

Figure 4.7: Color change on the addition of **(A)** 20-600 µL of Hg^{2+} **(B)** 25-80 µL of Hg^{2+}

When 20 µL of Hg^{2+} was added, the solution held a light yellow color, but when 50 µL or more of Hg^{2+} solution was added in the first phase of the experiment, as shown in figure 4.7 (A), the solution became colorless.

The experiment's second step involved the addition of various quantities ranging from 25 to 80 µL. AgNPs dispersion turned completely colorless when 45µL of Hg^{2+} solution was added, demonstrating the sensing scale of the AgNPs as shown in Figure 4.8 (B).

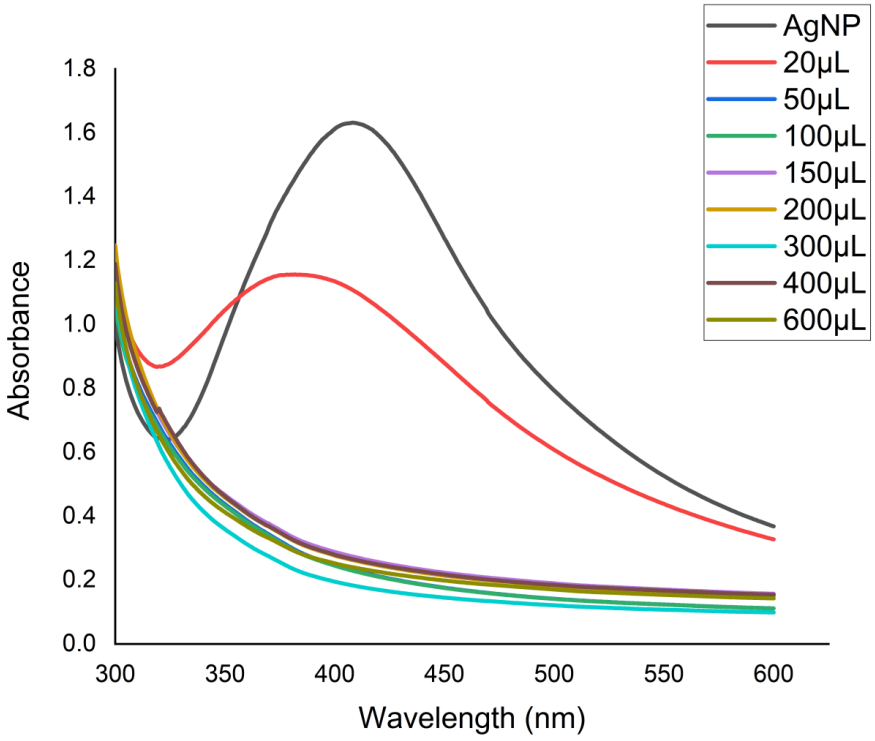

(A)

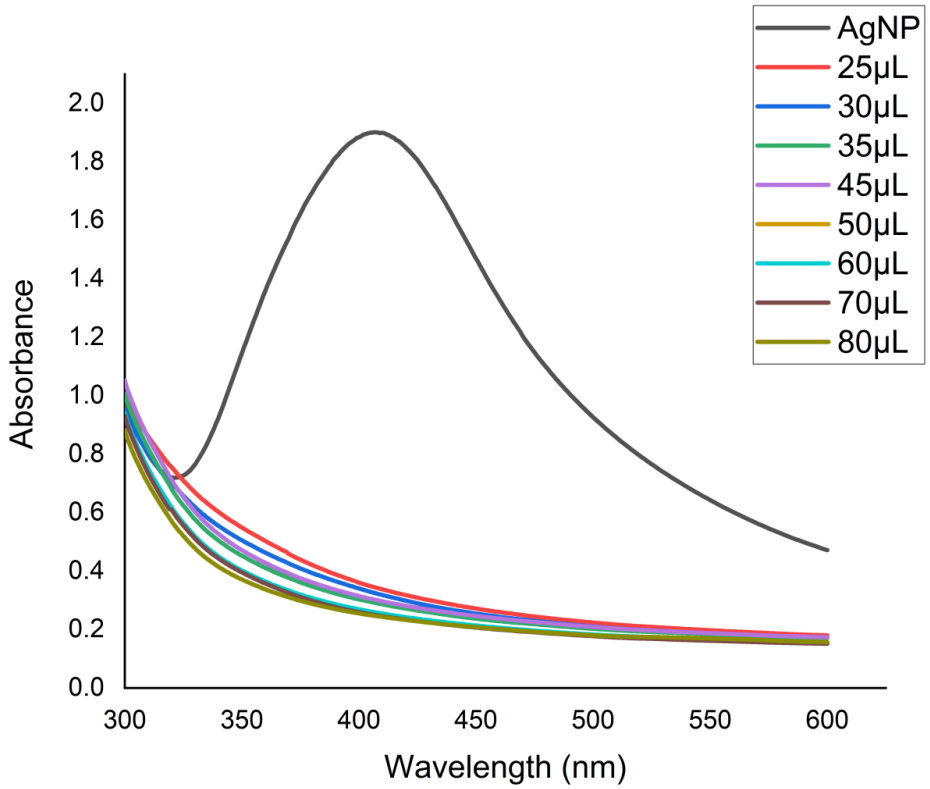

(B)

Figure 4.8: UV-Vis Spectra of Silver nanoparticles with **(A)** 20-800 µL of Hg^{2+} **(B)** 25-80µL of Hg^{2+}

After adding various amounts of Hg^{2+} ion solutions, the UV-Vis spectra were captured. As shown in Figure 4.8 (A), it proved that the SPR band blue-shifted with decreasing peak strength and broadened with increasing Hg^{2+} ion solution volume. After the addition of the 30 µL and greater volume of Hg^{2+} solution, the AgNPs SPR band vanished as in Figure 4.8(B).

It is conceivable that the outcome is the result of a redox reaction between Hg^{2+} and Ag^{+}. Hg^{2+} has a tendency to oxidize to Ag^{+} due to its larger reduction potential, i.e ($E^{0}_{Hg2+/Hg}$ =+ 0.80V) than Ag^{0} ($E^{0}_{Ag+/Ag}$ = +0.85V)[105]. The reaction between AgNPs and Hg^{2+} produced metallic mercury. By radiolytically generating an amalgam or another protective covering around the silver particle, the SPR band widened and the blue shift took place. On the surface of silver, the freshly produced metallic mercury could provide a strong bond.

4.3.2 Photocatalytic Degradation of Methylene Blue

The methylene blue of 10 ppm concentration has intense color before adding AgNPs and H_2O_2. With the addition of 0.5 mL H_2O_2 and 1 mL AgNPs to the MB solution, the blue color of the solution fades away to some extent. In this work, the oxidative degradation of Methylene blue was tested using produced silver nanoparticles.

In the figure above, the UV spectrum of Methylene blue with AgNPs and hydrogen peroxide solution is recorded in different time intervals of 0 min, 20 min, 40 min, 60 min and so on with continuous sunlight.

The methylene blue dye's initial 603 nm absorption peaks slowly decreased with increasing exposure duration, which points to methylene blue's photocatalytic degradation reaction. Methylene blue dye's absorption peak was lowered, absorption band for AgNPs was increased. The progressive decrease in the absorbance value of the dye approaching the baseline and an enhanced peak indicate that the photocatalytic degradation of the dyes is occured. The percentage of degradation efficiency of AgNPs at 140 min was calculated as 85.39%. As the dye AgNPs complex was exposed to sunlight for longer periods, the degradation percentage emerged. It is reported that absorption peak for methylene blue dye was centered at 660 nm in noticeable region which diminished and in the end, it disappeared while increasing the reaction time, which demonstrates that the dye had been degraded (Vanaja et al., 2014). The methylene blue dye's absorption peak cantered at 603 nm in the noticeable area, but as the reaction time increased, the peak decreased until it eventually disappeared proving that the dye experienced degradation which is confirmed by the reported article.

$$Efficiency\ (\%) = \frac{Ao - A}{Ao} * 100$$

In which efficiency (%) represents the degradation efficiency of dye.

A_0= absorbance of dye solution at zero time.

A= absorbance of dye solution in suspension after time t.

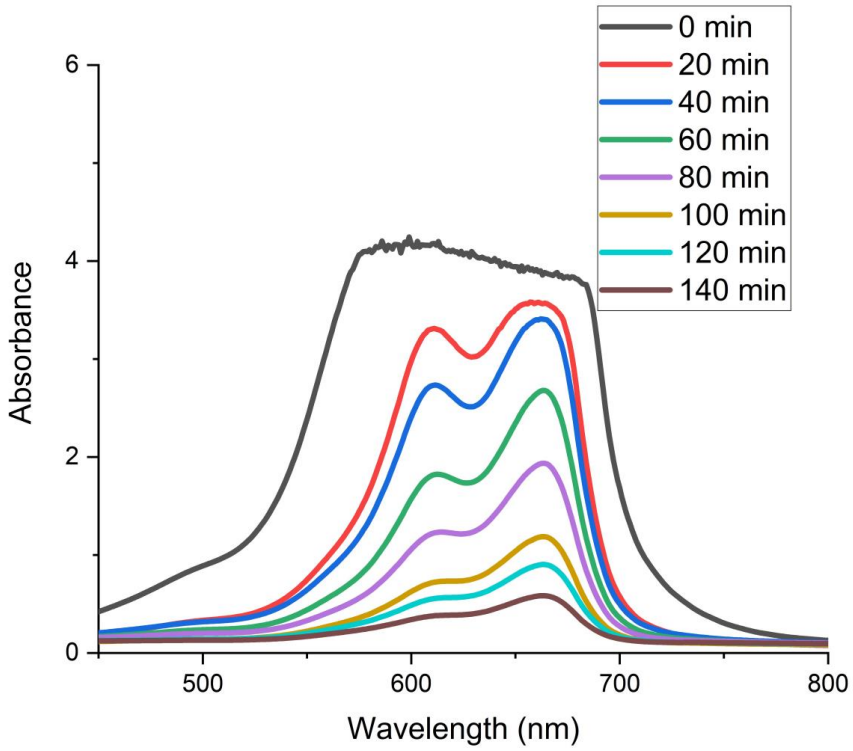

Figure4.9: UV-Vis absorption at different time of methylene blue in presence of AgNPs

Table 4.2: Calculation dye degradation efficiency of methylene blue by synthesized AgNPs

Time (min)	Maximum absorbance	Degradation (%)
0	3.85286	0
20	3.56367	7.50592
40	3.40719	11.56732
60	2.68421	30.332
80	1.94737	49.45655
100	1.18874	69.14661
120	0.89955	76.65248
140	0.56282	85.39219

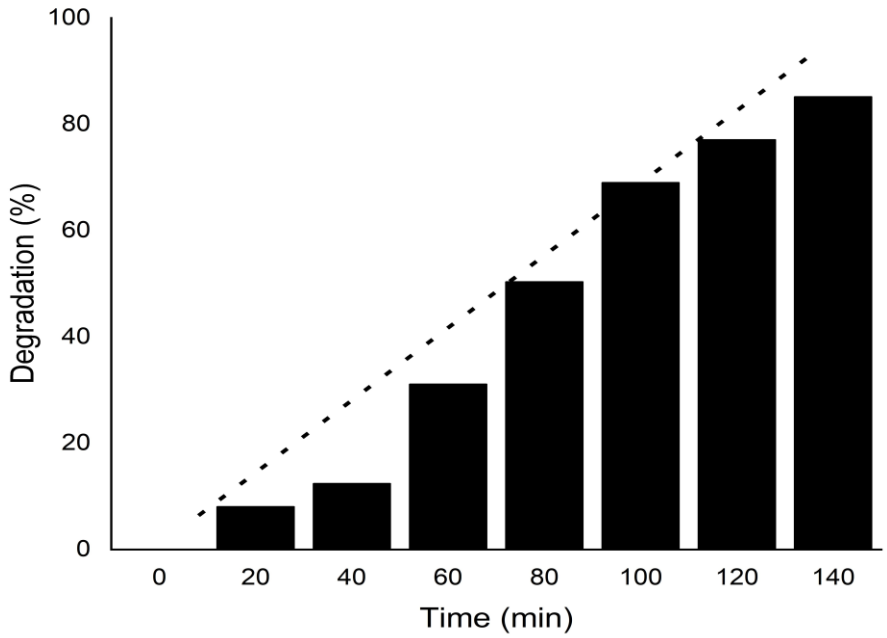

Figure 4.10: Graphical representation of degradation of methylene blue by AgNPs

4.3.3 Photocatalytic Degradation of Methyl Orange (MO)

The methyl orange (MO) of 10 ppm concentration has intense color before adding AgNPs and H_2O_2. With the addition of 0.5 mL H_2O_2 and 1 mL AgNPs to the MO solution, the dark orange color of the solution vanish away to some extent. This experiment tested if synthesized AgNPs could help MO oxidatively degrade.

In the figure 4.11, the UV spectrum of MO with AgNPs and hydrogen peroxide solution is recorded in different time intervals of 0 min, 20 min, 40 min, 60 min and so on with continuous sunlight. Using a sun irradiation approach and biometrically generated AgNPs at various time intervals, the photocatalytic degradation of the color MO was studied. It has been found that the methyl orange solution's characteristic absorption peak measured at 460 nm. Within 2 hours of incubation, a decrease in peak intensity allowed researchers to see the degradation of MO. Without exposure to AgNPs, the peak position of the MO solution is not altered significantly. According to Kansal and coworkers, solar light decolorized methyl orange more quickly than other irradiation methods when there was a metal catalyst involved (Kansal et al., 2008). Ag nanoparticle adsorption on the MO solution started slowly and then gradually increased over time.

Overall, the excitation of SPR, which is nothing more than an oscillation of charge density that can circulate at the interface between metal and dielectric media, may be the reason for AgNPs visible light photocatalytic activities (Garcia, 2011). According to Wang and his coworker, under ambient temperature and apparent light illumination, AgNPs work well as dyes and organic compound photocatalysts because they are highly effective and stable (Wang et al., 2008).

$$Efficiency\ (\%) = \frac{Ao - A}{Ao} * 100$$

In which efficiency (%) represents the degradation efficiency of dye.

A_0= absorbance of dye solution at zero time.

A= absorbance of dye solution in suspension after time t.

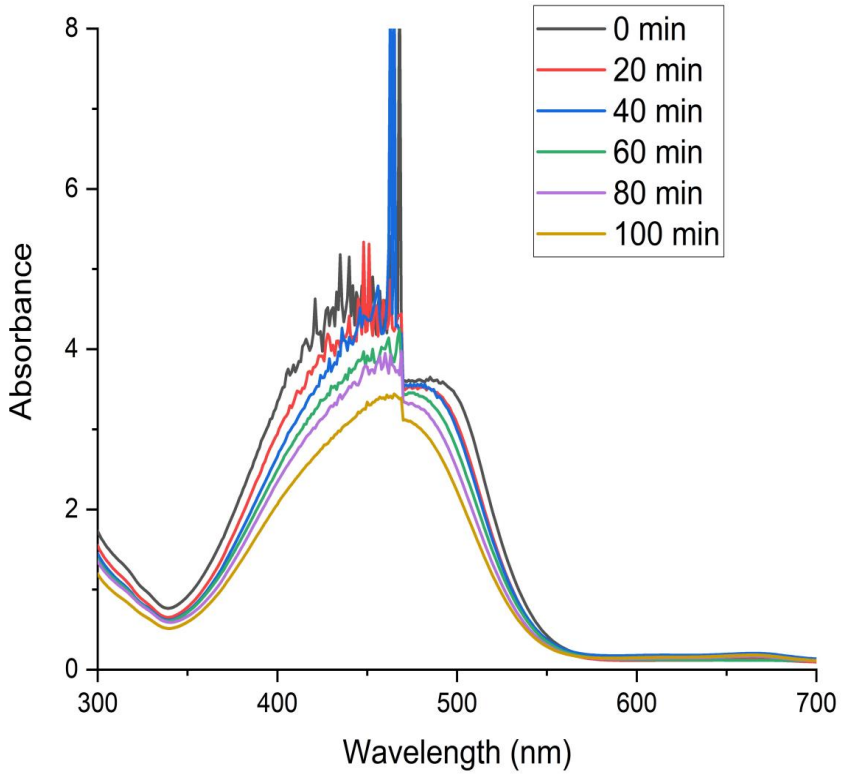

Figure 4.11: UV-Vis absorption at different times of methyl orange in the presence of AgNPs

Table 4.3: Calculation of degradation efficiency of MO by synthesized AgNPs

Time (min)	Maximum absorbance	Degradation (%)
0	4.83701	0
20	4.618	4.52787
40	4.32513	10.58263
60	3.90492	19.26989
80	3.73684	22.74479
100	3.33192	31.11615

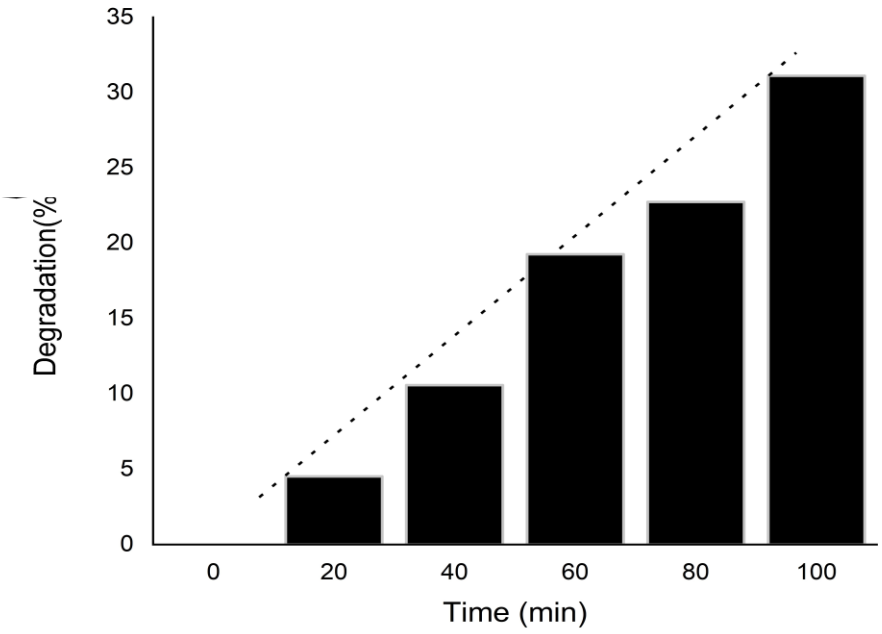

Figure 4.12: Graphical representation methyl orange degradation by AgNPs

4.3.4 Detection of Formaldehyde

In the experiment, five samples of formaldehyde with different percentage concentrations were subjected to the observation for colorimetric sensing. The observation was carried out with 40%, 30%, 20%, 10%, and 1% formaldehyde solution.

At first, the color of the formaldehyde in all concentrations is clear and transparent i.e. no color. In the experiment, after the addition of silver nanoparticles resulting alteration

occurs respectively. In the beginning, the color 1% of formaldehyde becomes yellowish red color and likewise, 10%, 20%, and 30% formaldehyde solution fade in the color from yellowish red and in the 40% solution it turns to little yellow .That alteration in the color of formaldehyde into different colors indicates the change in LSPR properties of AgNPs which is because of the interaction of the electromagnetic radiation and the electrons on the surface of AgNPs (Proposition et al., 2020). And, in 40% there will higher concentration of formaldehyde and in 1% will be a lesser concentration of formaldehyde and color changes likewise.

After the observation of the color change of the formaldehyde solution, all the resulting solutions were subjected to a UV-Visible spectrophotometer and absorbance was measured, and results obtained is shown in figure 4.13.

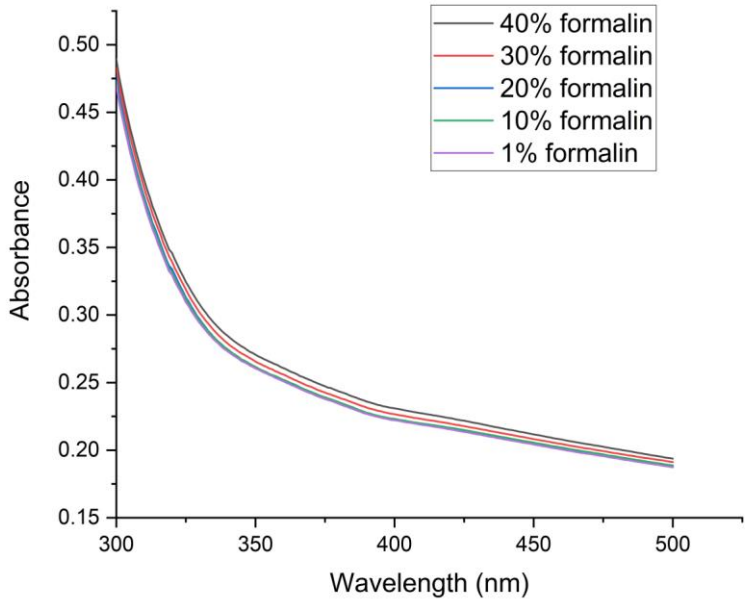

Figure 4.13(A): UV spectra of different formaldehyde without AgNPs

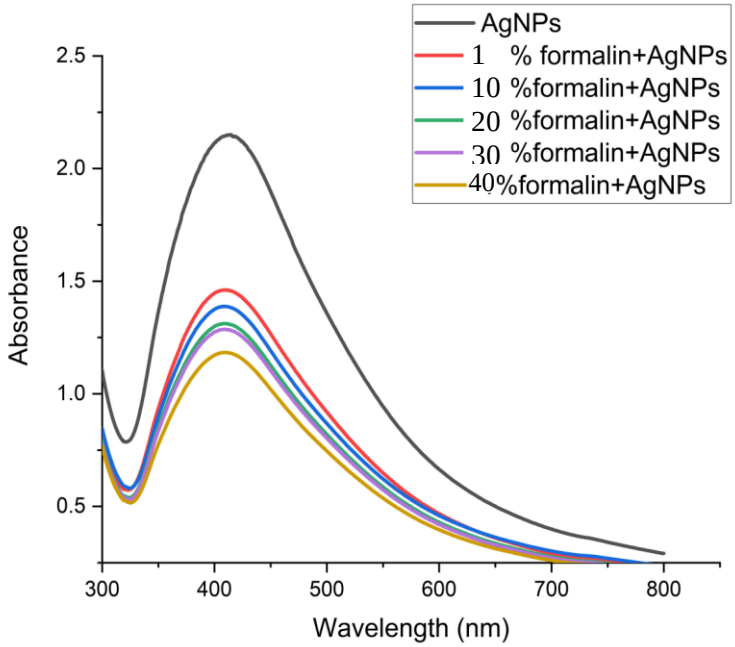

Figure 4.13 (B): UV spectra after adding AgNPs

In the figure above, UV spectra of different percentage concentration solutions of formaldehyde without AgNPs are recorded and it is observed that there is no significant peak in the range of 400nm- 500nm i.e., of the peak range of AgNPs. After the addition of AgNPs in (figure 4.13(B), the peak intensity is highest for the AgNPs without formaldehyde then after 1% formaldehyde + AgNPs solution and accordingly decrease the intensity of the resulting mixture and finally 40% formaldehyde + AgNPs solution gives the lowest peak in comparison to other because of the aggregation of the nanoparticles by formaldehyde and very less amount of nanoparticle is present in that solution. In 1% formaldehyde + AgNPs solution, there is a less amount of formaldehyde concentration and less no of silver aggregated and shows an intense peak comparatively than that of other solutions. This change in color and peak absorbance is because of the interaction between the formaldehyde solution and AgNPs (Qin et al., 2018). Higher the concentration of formaldehyde, the lesser the peak intensity, and the lower the concentration of formaldehyde, the higher the peak intensity or absorbance.

CHAPTER V

5 CONCLUSION

The present study concluded that the green synthesis of AgNPs, *C. longa* extract as reducing and capping agent, having advantages such as, ease in availability, ecofriendly with which the process can be scaled up economic viability. The secondary metabolites were responsible in the green synthesis of AgNPs. To elucidate precise mechanism and to comprehend the entire procedure behind green synthesis of silver NPs, further study is required. The formation of AgNPs were further characterized by FTIR and XRD that also revealed the formation of AgNPs. The biosynthesized nanoparticle showed the good sensing activity towards Hg^{2+}. Moreover, IONPs showed excellent photocatalytic organic dye degradation efficiency of 85.39 % and 31.11% in 140 minutes and 100 minutes, for methylene blue and methyl orange respectively. The synthesized AgNPs exhibited the good sensing property in different concentration of formaldehyde. Therefore, green synthesized AgNPs could be employed to detect the hazardous Hg^{2+} ion in aqueous medium to save the environment from mercury pollution and in catalytic reduction of organic dyes.

The present research work leaves the following future prospects.

- Further optimization of protocol (effect of temperature, $AgNO_3$, concentration, plant extracts concentration) is necessary for the large scale production of AgNPs.
- Comprehensive study is required to prepare the AgNps based sensor and application in catalysis.
- The toxicity should be tested for commercialization of the AgNPs.
- Besides the study of sensing and catalytic activity of AgNPs, other properties and their possible application should be studied.

REFERENCES

Acosta, E. J., Gonzalez, S. O., & Simanek, E. E. (2005). Synthesis, characterization, and application of melamine-based dendrimers supported on silica gel. *Journal of Polymer Science Part A: Polymer Chemistry*, *43*(1), 168–177. https://doi.org/10.1002/pola.20493

Ahmad, A., Wei, Y., Syed, F., Tahir, K., Rehman, A. U., Khan, A., Ullah, S., & Yuan, Q. (2017). The effects of bacteria-nanoparticles interface on the antibacterial activity of green synthesized silver nanoparticles. *Microbial Pathogenesis*, *102*, 133–142. https://doi.org/10.1016/j.micpath.2016.11.030

Ahmed, S., Ahmad, M., Swami, B. L., & Ikram, S. (2016a). A review on plants extract mediated synthesis of silver nanoparticles for antimicrobial applications: A green expertise. *Journal of Advanced Research*, *7*(1), 17–28. https://doi.org/10.1016/j.jare.2015.02.007

Ahmed, S., Ahmad, M., Swami, B. L., & Ikram, S. (2016b). A review on plants extract mediated synthesis of silver nanoparticles for antimicrobial applications: A green expertise. *Journal of Advanced Research*, *7*(1), 17–28. https://doi.org/10.1016/j.jare.2015.02.007

Ahmed, S., Annu, Ikram, S., & Yudha S., S. (2016). Biosynthesis of gold nanoparticles: A green approach. *Journal of Photochemistry and Photobiology B: Biology*, *161*, 141–153. https://doi.org/10.1016/j.jphotobiol.2016.04.034

Ahmed, S., Saifullah, Ahmad, M., Swami, B. L., & Ikram, S. (2016). Green synthesis of silver nanoparticles using Azadirachta indica aqueous leaf extract. *Journal of Radiation Research and Applied Sciences*, *9*(1), 1–7. https://doi.org/10.1016/j.jrras.2015.06.006

Ajitha, B., Ashok Kumar Reddy, Y., Shameer, S., Rajesh, K. M., Suneetha, Y., & Sreedhara Reddy, P. (2015). Lantana camara leaf extract mediated silver nanoparticles: Antibacterial, green catalyst. *Journal of Photochemistry and Photobiology B: Biology*, *149*, 84–92. https://doi.org/10.1016/j.jphotobiol.2015.05.020

Akpolat, M., Kamat, B., Gülle, K., & Bakkal, B. H. (2018). Skrotal Radyoterapide Curcuminin Profilaktik Kullanımı Testis Dokusunda PARP-1 İmmünreaktivitesini ve Spermatogenezi Nasıl Etkiler? *SDÜ Tıp Fakültesi Dergisi*, *25*(4), Article 4. https://doi.org/10.17343/sdutfd.387496

Ali, S. M., Yousef, N. M. H., & Nafady, N. A. (2015). Application of Biosynthesized Silver Nanoparticles for the Control of Land Snail *Eobania vermiculata* and Some Plant Pathogenic Fungi. *Journal of Nanomaterials*, *2015*, e218904. https://doi.org/10.1155/2015/218904

Alsammarraie, F. K., Wang, W., Zhou, P., Mustapha, A., & Lin, M. (2018). Green synthesis of silver nanoparticles using turmeric extracts and investigation of their antibacterial activities. *Colloids and Surfaces B: Biointerfaces*, *171*, 398–405. https://doi.org/10.1016/j.colsurfb.2018.07.059

Alvarez, D. A., Corsi, S. R., De Cicco, L. A., Villeneuve, D. L., & Baldwin, A. K. (2021). Identifying Chemicals and Mixtures of Potential Biological Concern Detected in Passive Samplers from Great Lakes Tributaries Using High-Throughput Data and Biological Pathways. *Environmental Toxicology and Chemistry*, *40*(8), 2165–2182. https://doi.org/10.1002/etc.5118

Anandalakshmi, K., Venugobal, J., & Ramasamy, V. (2016). Characterization of silver nanoparticles by green synthesis method using Pedalium murex leaf extract and their antibacterial activity. *Applied Nanoscience*, *6*(3), 399–408. https://doi.org/10.1007/s13204-015-0449-z

Ananias, D., Almeida Paz, F. A., Carlos, L. D., & Rocha, J. (2013). Chiral microporous rare-earth silico-germanates: Synthesis, structure and photoluminescence properties. *Microporous and Mesoporous Materials*, *166*, 50–58. https://doi.org/10.1016/j.micromeso.2012.04.032

Ankamwar, B., Damle, C., Ahmad, A., & Sastry, M. (2005). Biosynthesis of Gold and Silver Nanoparticles Using Emblica Officinalis Fruit Extract, Their Phase Transfer and Transmetallation in an Organic Solution. *Journal of Nanoscience and Nanotechnology*, *5*(10), 1665–1671. https://doi.org/10.1166/jnn.2005.184

Asti, M., Ferrari, E., Croci, S., Atti, G., Rubagotti, S., Iori, M., Capponi, P. C., Zerbini, A., Saladini, M., & Versari, A. (2014). Synthesis and Characterization of 68Ga-Labeled Curcumin and Curcuminoid Complexes as Potential Radiotracers for Imaging of Cancer and Alzheimer's Disease. *Inorganic Chemistry*, *53*(10), 4922–4933. https://doi.org/10.1021/ic403113z

Banerjee, K., Das, S., Choudhury, P., Ghosh, S., Baral, R., & Choudhuri, S. K. (2017). A Novel Approach of Synthesizing and Evaluating the Anticancer Potential of Silver Oxide Nanoparticles in vitro. *Chemotherapy*, *62*(5), 279–289. https://doi.org/10.1159/000453446

Banthia, S., & Samanta, A. (2005). A two-dimensional chromogenic sensor as well as fluorescence inverter: Selective detection of copper(II) in aqueous medium. *New Journal of Chemistry*, *29*(8), 1007–1010. https://doi.org/10.1039/B504823K

Barman, G., Maiti, S., & Laha, J. K. (2013). Bio-fabrication of gold nanoparticles using aqueous extract of red tomato and its use as a colorimetric sensor. *Nanoscale Research Letters*, *8*(1), 181. https://doi.org/10.1186/1556-276X-8-181

Barth, A., & Zscherp, C. (2002). What vibrations tell about proteins. *Quarterly Reviews of Biophysics*, *35*(4), 369–430. https://doi.org/10.1017/S0033583502003815

Baudot, C., Tan, C. M., & Kong, J. C. (2010). FTIR spectroscopy as a tool for nano-material characterization. *Infrared Physics & Technology*, *53*(6), 434–438. https://doi.org/10.1016/j.infrared.2010.09.002

Becker, J. S., Matusch, A., Depboylu, C., Dobrowolska, J., & Zoriy, M. V. (2007). Quantitative Imaging of Selenium, Copper, and Zinc in Thin Sections of Biological Tissues (Slugs−Genus Arion) Measured by Laser Ablation Inductively Coupled Plasma Mass Spectrometry. *Analytical Chemistry*, *79*(16), 6074–6080. https://doi.org/10.1021/ac0700528

Begum, N. A., Mondal, S., Basu, S., Laskar, R. A., & Mandal, D. (2009). Biogenic synthesis of Au and Ag nanoparticles using aqueous solutions of Black Tea leaf extracts. *Colloids and Surfaces. B, Biointerfaces*, *71*(1), 113–118. https://doi.org/10.1016/j.colsurfb.2009.01.012

Bhainsa, K. C., & D'Souza, S. F. (2006). Extracellular biosynthesis of silver nanoparticles using the fungus Aspergillus fumigatus. *Colloids and Surfaces B: Biointerfaces*, *47*(2), 160–164. https://doi.org/10.1016/j.colsurfb.2005.11.026

Bhattacharya, R., & Mukherjee, P. (2008). Biological properties of "naked" metal nanoparticles☆. *Advanced Drug Delivery Reviews*, *60*(11), 1289–1306. https://doi.org/10.1016/j.addr.2008.03.013

Biswas, A., Vanlalveni, C., Adhikari, P. P., Lalfakzuala, R., & Rokhum, L. (2018). Green biosynthesis, characterisation and antimicrobial activities of silver nanoparticles using fruit extract of Solanum viarum. *IET Nanobiotechnology*, *12*(7), 933–938. https://doi.org/10.1049/iet-nbt.2018.0050

Buffat, Ph., & Borel, J.-P. (1976). Size effect on the melting temperature of gold particles. *Physical Review A*, *13*(6), 2287–2298. https://doi.org/10.1103/PhysRevA.13.2287

Buzea, C., Pacheco, I. I., & Robbie, K. (2007). Nanomaterials and nanoparticles: Sources and toxicity. *Biointerphases*, *2*(4), MR17–MR71. https://doi.org/10.1116/1.2815690

Campbell, L., Dixon, D. G., & Hecky, R. E. (2003). A Review Of Mercury in Lake Victoria, East Africa: Implications for Human and Ecosystem Health. *Journal of Toxicology and Environmental Health, Part B*, *6*(4), 325–356. https://doi.org/10.1080/10937400306474

Carvalho Oliveira Cambrussi, A. N., de Sena Neto, L. R., da Silva Filho, E. C., Anteveli Furtini Osajima, J., & Braga Ribeiro, A. (2019). Heterogeneous photocatalysis using TiO2 in suspension applied to antioxidant activity assays. *Materials Today: Proceedings*, *14*, 648–655. https://doi.org/10.1016/j.matpr.2019.02.002

Cassie, A. B. D., & Baxter, S. (1944). Wettability of porous surfaces. *Transactions of the Faraday Society*, *40*(0), 546–551. https://doi.org/10.1039/TF9444000546

Castro-Longoria, E., Vilchis-Nestor, A. R., & Avalos-Borja, M. (2011). Biosynthesis of silver, gold and bimetallic nanoparticles using the filamentous fungus Neurospora crassa. *Colloids and Surfaces. B, Biointerfaces*, *83*(1), 42–48. https://doi.org/10.1016/j.colsurfb.2010.10.035

Chandraker, S. K., Ghosh, M. K., Lal, M., Ghorai, T. K., & Shukla, R. (2019). Colorimetric sensing of Fe3+ and Hg2+ and photocatalytic activity of green synthesized silver nanoparticles from the leaf extract of Sonchus arvensis L. *New Journal of Chemistry*, *43*(46), 18175–18183. https://doi.org/10.1039/C9NJ01338E

Changmai, B., Laskar, I. B., & Rokhum, S. L. (2019). Microwave-assisted synthesis of glycerol carbonate by the transesterification of glycerol with dimethyl carbonate using Musa acuminata peel ash catalyst. *Journal of the Taiwan Institute of Chemical Engineers*, *102*, 276–282. https://doi.org/10.1016/j.jtice.2019.06.014

Changmai, B., Sudarsanam, P., & Rokhum, S. L. (2020). Biodiesel production using a renewable mesoporous solid catalyst. *Industrial Crops and Products*, *145*, 111911. https://doi.org/10.1016/j.indcrop.2019.111911

Choi, Y.-J., & Park, H.-H. (2011). Direct patterning of SnO2 composite films prepared with various contents of Pt nanoparticles by photochemical metal-organic deposition. *Thin Solid Films*, *519*(19), 6214–6218. https://doi.org/10.1016/j.tsf.2011.03.051

Christopher, V., Roy, A., & Shanmugam, R. (2021). Turmeric Oil Mediated Green Synthesis of Silver Nanoparticles and their Antioxidant Activity. *Journal of Evolution of Medical and Dental Sciences*, *10*, 558–561. https://doi.org/10.14260/jemds/2021/121

Corbett, J., McKeown, P. A., Peggs, G. N., & Whatmore, R. (2000). Nanotechnology: International Developments and Emerging Products. *CIRP Annals*, *49*(2), 523–545. https://doi.org/10.1016/S0007-8506(07)63454-4

Daniel, M.-C., & Astruc, D. (2004). Gold Nanoparticles: Assembly, Supramolecular Chemistry, Quantum-Size-Related Properties, and Applications toward Biology, Catalysis, and Nanotechnology. *Chemical Reviews*, *104*(1), 293–346. https://doi.org/10.1021/cr030698+

Daniel, W. L., Han, M. S., Lee, J.-S., & Mirkin, C. A. (2009). Colorimetric Nitrite and Nitrate Detection with Gold Nanoparticle Probes and Kinetic End Points.

Journal of the American Chemical Society, *131*(18), 6362–6363. https://doi.org/10.1021/ja901609k

Das, R. K., Pachapur, V. L., Lonappan, L., Naghdi, M., Pulicharla, R., Maiti, S., Cledon, M., Dalila, L. M. A., Sarma, S. J., & Brar, S. K. (2017). Biological synthesis of metallic nanoparticles: Plants, animals and microbial aspects. *Nanotechnology for Environmental Engineering*, *2*(1), 18. https://doi.org/10.1007/s41204-017-0029-4

Desimoni, E., & Brunetti, B. (2015). X-Ray Photoelectron Spectroscopic Characterization of Chemically Modified Electrodes Used as Chemical Sensors and Biosensors: A Review. *Chemosensors*, *3*(2), Article 2. https://doi.org/10.3390/chemosensors3020070

Devanesan, S., Ponmurugan, K., AlSalhi, M. S., & Al-Dhabi, N. A. (2020). Cytotoxic and Antimicrobial Efficacy of Silver Nanoparticles Synthesized Using a Traditional Phytoproduct, Asafoetida Gum . *International Journal of Nanomedicine*, *15*, 4351–4362. https://doi.org/10.2147/IJN.S258319

Dey, A., Mukhopadhyay, A. K., Gangadharan, S., Sinha, M. K., & Basu, D. (2009). Characterization of Microplasma Sprayed Hydroxyapatite Coating. *Journal of Thermal Spray Technology*, *18*(4), 578–592. https://doi.org/10.1007/s11666-009-9386-2

Dhand, V., Soumya, L., Bharadwaj, S., Chakra, S., Bhatt, D., & Sreedhar, B. (2016). Green synthesis of silver nanoparticles using Coffea arabica seed extract and its antibacterial activity. *Materials Science and Engineering: C*, *58*, 36–43. https://doi.org/10.1016/j.msec.2015.08.018

Dieckmann, Y., Cölfen, H., Hofmann, H., & Petri-Fink, A. (2009). Particle Size Distribution Measurements of Manganese-Doped ZnS Nanoparticles. *Analytical Chemistry*, *81*(10), 3889–3895. https://doi.org/10.1021/ac900043y

Díez, A. M., Moreira, F. C., Marinho, B. A., Espíndola, J. C. A., Paulista, L. O., Sanromán, M. A., Pazos, M., Boaventura, R. A. R., & Vilar, V. J. P. (2018). A step forward in heterogeneous photocatalysis: Process intensification by using

a static mixer as catalyst support. *Chemical Engineering Journal*, *343*, 597–606. https://doi.org/10.1016/j.cej.2018.03.041

Dolatmoradi, A., Raygan, S., & Abdizadeh, H. (2013). Mechanochemical synthesis of W–Cu nanocomposites via in-situ co-reduction of the oxides. *Powder Technology*, *233*, 208–214. https://doi.org/10.1016/j.powtec.2012.08.013

Dong, H., Wen, B., & Melnik, R. (2014). Relative importance of grain boundaries and size effects in thermal conductivity of nanocrystalline materials. *Scientific Reports*, *4*(1), Article 1. https://doi.org/10.1038/srep07037

Drake, P. L., & Hazelwood, K. J. (2005). Exposure-related health effects of silver and silver compounds: A review. *The Annals of Occupational Hygiene*, *49*(7), 575–585. https://doi.org/10.1093/annhyg/mei019

EL-Kenawy, A. E.-M., Hassan, S. M. A., Mohamed, A. M. M., & Mohammed, H. M. A. (2019). Chapter 3.43—Tumeric or Curcuma longa Linn. In S. M. Nabavi & A. S. Silva (Eds.), *Nonvitamin and Nonmineral Nutritional Supplements* (pp. 447–453). Academic Press. https://doi.org/10.1016/B978-0-12-812491-8.00059-X

El-Shanshoury, A. E.-R. R., ElSilk, S. E., & Ebeid, M. E. (2011). Extracellular Biosynthesis of Silver Nanoparticles Using *Escherichia coli* ATCC 8739, *Bacillus subtilis* ATCC 6633, and *Streptococcus thermophilus* ESh1 and Their Antimicrobial Activities. *International Scholarly Research Notices*, *2011*, e385480. https://doi.org/10.5402/2011/385480

Erenler, R., Geçer, E. N., Genç, N., & Yanar, D. (2021). Antioxidant activity of silver nanoparticles synthesized from Tagetes erecta L. leaves. *International Journal of Chemistry and Technology*, *5*(2), Article 2. https://doi.org/10.32571/ijct.1005275

Fan, Y., Liu, Z., Wang, L. e., & Zhan, J. (2009). Synthesis of Starch-Stabilized Ag Nanoparticles and Hg2+Recognition in Aqueous Media. *Nanoscale Research Letters*, *4*(10), 1230. https://doi.org/10.1007/s11671-009-9387-6

Feynman, R. P. (n.d.). *Plenty of Room at the Bottom*.

Fissan, H., Ristig, S., Kaminski, H., Asbach, C., & Epple, M. (2014). Comparison of different characterization methods for nanoparticle dispersions before and after aerosolization. *Analytical Methods*, *6*(18), 7324–7334. https://doi.org/10.1039/C4AY01203H

Furst, A., & Schlauder, M. C. (1978). Inactivity of two noble metals as carcinogens. *Journal of Environmental Pathology and Toxicology*, *1*(1), 51–57.

Garcia, M. A. (2011). Surface plasmons in metallic nanoparticles: Fundamentals and applications. *Journal of Physics D: Applied Physics*, *44*(28), 283001. https://doi.org/10.1088/0022-3727/44/28/283001

Gardea-Torresdey, J. L., Parsons, J. G., Gomez, E., Peralta-Videa, J., Troiani, H. E., Santiago, P., & Yacaman, M. J. (2002). Formation and Growth of Au Nanoparticles inside Live Alfalfa Plants. *Nano Letters*, *2*(4), 397–401. https://doi.org/10.1021/nl015673+

Gaya, U. I., & Abdullah, A. H. (2008). Heterogeneous photocatalytic degradation of organic contaminants over titanium dioxide: A review of fundamentals, progress and problems. *Journal of Photochemistry and Photobiology C: Photochemistry Reviews*, *9*(1), 1–12. https://doi.org/10.1016/j.jphotochemrev.2007.12.003

Gerwert, K. (1999). *Molecular Reaction Mechanisms of Proteins Monitored by Time-Resolved FTIR-Spectroscopy*. *380*(7–8), 931–935. https://doi.org/10.1515/BC.1999.115

Ghosh, S. K., Kundu, S., Mandal, M., & Pal, T. (2002). Silver and Gold Nanocluster Catalyzed Reduction of Methylene Blue by Arsine in a Micellar Medium. *Langmuir*, *18*(23), 8756–8760. https://doi.org/10.1021/la0201974

Gole, A., Dash, C., Ramakrishnan, V., Sainkar, S. R., Mandale, A. B., Rao, M., & Sastry, M. (2001). Pepsin−Gold Colloid Conjugates: Preparation, Characterization, and Enzymatic Activity. *Langmuir*, *17*(5), 1674–1679. https://doi.org/10.1021/la001164w

Gomez-Romero, P. (2001). Hybrid Organic–Inorganic Materials—In Search of Synergic Activity. *Advanced Materials*, *13*(3), 163–174.

https://doi.org/10.1002/1521-4095(200102)13:3<163::AID-ADMA163>3.0.CO;2-U

Gonçalves, N. P. F., Paganini, M. C., Armillotta, P., Cerrato, E., & Calza, P. (2019). The effect of cobalt doping on the efficiency of semiconductor oxides in the photocatalytic water remediation. *Journal of Environmental Chemical Engineering*, *7*(6), 103475. https://doi.org/10.1016/j.jece.2019.103475

Goormaghtigh, E., Raussens, V., & Ruysschaert, J. M. (1999). Attenuated total reflection infrared spectroscopy of proteins and lipids in biological membranes. *Biochimica Et Biophysica Acta*, *1422*(2), 105–185. https://doi.org/10.1016/s0304-4157(99)00004-0

Gupta, A., Briffa, S. M., Swingler, S., Gibson, H., Kannappan, V., Adamus, G., Kowalczuk, M., Martin, C., & Radecka, I. (2020). Synthesis of Silver Nanoparticles Using Curcumin-Cyclodextrins Loaded into Bacterial Cellulose-Based Hydrogels for Wound Dressing Applications. *Biomacromolecules*, *21*(5), 1802–1811. https://doi.org/10.1021/acs.biomac.9b01724

Gupta, A., Keddie, D. J., Kannappan, V., Gibson, H., Khalil, I. R., Kowalczuk, M., Martin, C., Shuai, X., & Radecka, I. (2019). Production and characterisation of bacterial cellulose hydrogels loaded with curcumin encapsulated in cyclodextrins as wound dressings. *European Polymer Journal*, *118*, 437–450. https://doi.org/10.1016/j.eurpolymj.2019.06.018

Haefeli, C., Franklin, C., & Hardy, K. (1984). Plasmid-determined silver resistance in Pseudomonas stutzeri isolated from a silver mine. *Journal of Bacteriology*, *158*(1), 389–392. https://doi.org/10.1128/jb.158.1.389-392.1984

Hall, J. B., Dobrovolskaia, M. A., Patri, A. K., & McNeil, S. E. (2007). Characterization of nanoparticles for therapeutics. *Nanomedicine*, *2*(6), 789–803. https://doi.org/10.2217/17435889.2.6.789

Hamad, S., Podagatlapalli, G. K., Mohiddon, Md. A., & Soma, V. R. (2014). Cost effective nanostructured copper substrates prepared with ultrafast laser pulses for explosives detection using surface enhanced Raman scattering. *Applied Physics Letters*, *104*(26), 263104. https://doi.org/10.1063/1.4885763

Harrick, N. J., & Beckmann, K. H. (1974). Internal Reflection Spectroscopy. In P. F. Kane & G. B. Larrabee (Eds.), *Characterization of Solid Surfaces* (pp. 215–245). Springer US. https://doi.org/10.1007/978-1-4613-4490-2_11

He, R., Qian, X., Yin, J., & Zhu, Z. (2002). Preparation of polychrome silver nanoparticles in different solvents. *Journal of Materials Chemistry*, *12*(12), 3783–3786. https://doi.org/10.1039/B205214H

Henglein, A. (1993). Physicochemical properties of small metal particles in solution: "microelectrode" reactions, chemisorption, composite metal particles, and the atom-to-metal transition. *The Journal of Physical Chemistry*, *97*(21), 5457–5471. https://doi.org/10.1021/j100123a004

Hind, A. R., Bhargava, S. K., & McKinnon, A. (2001). At the solid/liquid interface: FTIR/ATR — the tool of choice. *Advances in Colloid and Interface Science*, *93*(1), 91–114. https://doi.org/10.1016/S0001-8686(00)00079-8

Hoang, C. V., Oyama, M., Saito, O., Aono, M., & Nagao, T. (2013). Monitoring the Presence of Ionic Mercury in Environmental Water by Plasmon-Enhanced Infrared Spectroscopy. *Scientific Reports*, *3*(1), Article 1. https://doi.org/10.1038/srep01175

Huang, X., Jain, P. K., El-Sayed, I. H., & El-Sayed, M. A. (2007). Gold nanoparticles: Interesting optical properties and recent applications in cancer diagnostics and therapy. *Nanomedicine (London, England)*, *2*(5), 681–693. https://doi.org/10.2217/17435889.2.5.681

Inagaki, S., Ghirlando, R., & Grisshammer, R. (2013). Biophysical characterization of membrane proteins in nanodiscs. *Methods*, *59*(3), 287–300. https://doi.org/10.1016/j.ymeth.2012.11.006

Jain, P. K., Huang, X., El-Sayed, I. H., & El-Sayed, M. A. (2008). Noble Metals on the Nanoscale: Optical and Photothermal Properties and Some Applications in Imaging, Sensing, Biology, and Medicine. *Accounts of Chemical Research*, *41*(12), 1578–1586. https://doi.org/10.1021/ar7002804

Janardhanan, A., Roshmi, T., Varghese, R., Soniya, E., Mathew, J., & Radhakrishnan, E. (2013). Biosynthesis of silver nanoparticles by a Bacillus sp. Of marine

origin. *Materials Science-Poland*, *31*(2), 173–179. https://doi.org/10.2478/s13536-012-0085-1

Jans, H., Liu, X., Austin, L., Maes, G., & Huo, Q. (2009). Dynamic Light Scattering as a Powerful Tool for Gold Nanoparticle Bioconjugation and Biomolecular Binding Studies. *Analytical Chemistry*, *81*(22), 9425–9432. https://doi.org/10.1021/ac901822w

Jha, A. K., Prasad, K., & Kulkarni, A. R. (2009). Synthesis of TiO2 nanoparticles using microorganisms. *Colloids and Surfaces. B, Biointerfaces*, *71*(2), 226–229. https://doi.org/10.1016/j.colsurfb.2009.02.007

Joerger, R., Klaus, T., & Granqvist, C. G. (2000). Biologically Produced Silver–Carbon Composite Materials for Optically Functional Thin-Film Coatings. *Advanced Materials*, *12*(6), 407–409. https://doi.org/10.1002/(SICI)1521-4095(200003)12:6<407::AID-ADMA407>3.0.CO;2-O

Jung, C. (2000). Insight into protein structure and protein–ligand recognition by Fourier transform infrared spectroscopy. *Journal of Molecular Recognition*, *13*(6), 325–351. https://doi.org/10.1002/1099-1352(200011/12)13:6<325::AID-JMR507>3.0.CO;2-C

Kannan, R. R. R., Arumugam, R., Ramya, D., Manivannan, K., & Anantharaman, P. (2013). Green synthesis of silver nanoparticles using marine macroalga Chaetomorpha linum. *Applied Nanoscience*, *3*(3), 229–233. https://doi.org/10.1007/s13204-012-0125-5

Kansal, S. K., Singh, M., & Sud, D. (2008). Studies on TiO2/ZnO photocatalysed degradation of lignin. *Journal of Hazardous Materials*, *153*(1), 412–417. https://doi.org/10.1016/j.jhazmat.2007.08.091

Kathiraven, T., Sundaramanickam, A., Shanmugam, N., & Balasubramanian, T. (2015). Green synthesis of silver nanoparticles using marine algae Caulerpa racemosa and their antibacterial activity against some human pathogens. *Applied Nanoscience*, *5*(4), 499–504. https://doi.org/10.1007/s13204-014-0341-2

Kazarian, S. G., & Chan, K. L. A. (2006). Applications of ATR-FTIR spectroscopic imaging to biomedical samples. *Biochimica et Biophysica Acta (BBA) - Biomembranes*, *1758*(7), 858–867. https://doi.org/10.1016/j.bbamem.2006.02.011

Kelly, K. L., Coronado, E., Zhao, L. L., & Schatz, G. C. (2003). The Optical Properties of Metal Nanoparticles: The Influence of Size, Shape, and Dielectric Environment. *The Journal of Physical Chemistry B*, *107*(3), 668–677. https://doi.org/10.1021/jp026731y

Khan, A., Asiri, A. M., Rub, M. A., Azum, N., Khan, A. A. P., Khan, S. B., Rahman, M. M., & Khan, I. (2013). Synthesis, characterization of silver nanoparticle embedded polyaniline tungstophosphate-nanocomposite cation exchanger and its application for heavy metal selective membrane. *Composites Part B: Engineering*, *45*(1), 1486–1492. https://doi.org/10.1016/j.compositesb.2012.09.023

Khan, M. J., Shameli, K., Sazili, A. Q., Selamat, J., & Kumari, S. (2019a). Rapid Green Synthesis and Characterization of Silver Nanoparticles Arbitrated by Curcumin in an Alkaline Medium. *Molecules*, *24*(4), Article 4. https://doi.org/10.3390/molecules24040719

Khan, M. J., Shameli, K., Sazili, A. Q., Selamat, J., & Kumari, S. (2019b). Rapid Green Synthesis and Characterization of Silver Nanoparticles Arbitrated by Curcumin in an Alkaline Medium. *Molecules*, *24*(4), Article 4. https://doi.org/10.3390/molecules24040719

Khan, S. U., Anjum, S. I., Ansari, M. J., Khan, M. H. U., Kamal, S., Rahman, K., Shoaib, M., Man, S., Khan, A. J., Khan, S. U., & Khan, D. (2019). Antimicrobial potentials of medicinal plant's extract and their derived silver nanoparticles: A focus on honey bee pathogen. *Saudi Journal of Biological Sciences*, *26*(7), 1815–1834. https://doi.org/10.1016/j.sjbs.2018.02.010

Khlebtsov, B. N., & Khlebtsov, N. G. (2011). On the measurement of gold nanoparticle sizes by the dynamic light scattering method. *Colloid Journal*, *73*(1), 118–127. https://doi.org/10.1134/S1061933X11010078

Kim, J. S., Kuk, E., Yu, K. N., Kim, J.-H., Park, S. J., Lee, H. J., Kim, S. H., Park, Y. K., Park, Y. H., Hwang, C.-Y., Kim, Y.-K., Lee, Y.-S., Jeong, D. H., & Cho, M.-H. (2007). Antimicrobial effects of silver nanoparticles. *Nanomedicine: Nanotechnology, Biology and Medicine*, *3*(1), 95–101. https://doi.org/10.1016/j.nano.2006.12.001

Kim, S., & Barry, B. A. (2001). Reaction-Induced FT-IR Spectroscopic Studies of Biological Energy Conversion in Oxygenic Photosynthesis and Transport. *The Journal of Physical Chemistry B*, *105*(19), 4072–4083. https://doi.org/10.1021/jp0042516

Kokila, T., Ramesh, P. S., & Geetha, D. (2015). Biosynthesis of silver nanoparticles from Cavendish banana peel extract and its antibacterial and free radical scavenging assay: A novel biological approach. *Applied Nanoscience*, *5*(8), 911–920. https://doi.org/10.1007/s13204-015-0401-2

Koppel, D. E. (2003). Analysis of Macromolecular Polydispersity in Intensity Correlation Spectroscopy: The Method of Cumulants. *The Journal of Chemical Physics*, *57*(11), 4814–4820. https://doi.org/10.1063/1.1678153

Kou, T., Jin, C., Zhang, C., Sun, J., & Zhang, Z. (2012). Nanoporous core–shell Cu@Cu2O nanocomposites with superior photocatalytic properties towards the degradation of methyl orange. *RSC Advances*, *2*(33), 12636–12643. https://doi.org/10.1039/C2RA21821F

Kouvaris, P., Delimitis, A., Zaspalis, V., Papadopoulos, D., Tsipas, S. A., & Michailidis, N. (2012). Green synthesis and characterization of silver nanoparticles produced using Arbutus Unedo leaf extract. *Materials Letters*, *76*, 18–20. https://doi.org/10.1016/j.matlet.2012.02.025

Kovatcheva, P. (n.d.). *LibGuides: Science - Biology 1 - Lab Reports Library Support: EXPERIMENT: Botany (Modified plant organs)*. Retrieved June 18, 2023, from https://uj.ac.za.libguides.com/biology/prac7

Królikowska, A., Kudelski, A., Michota, A., & Bukowska, J. (2003). SERS studies on the structure of thioglycolic acid monolayers on silver and gold. *Surface Science*, *532–535*, 227–232. https://doi.org/10.1016/S0039-6028(03)00094-3

Kumar, S., & Barth, A. (2010). Following Enzyme Activity with Infrared Spectroscopy. *Sensors*, *10*(4), Article 4. https://doi.org/10.3390/s100402626

Kyriacou, S. V., Brownlow, W. J., & Xu, X.-H. N. (2004). Using Nanoparticle Optics Assay for Direct Observation of the Function of Antimicrobial Agents in Single Live Bacterial Cells. *Biochemistry*, *43*(1), 140–147. https://doi.org/10.1021/bi0351110

Lange, H. (1995). Comparative Test of Methods to Determine Particle Size and Particle Size Distribution in the Submicron Range. *Particle & Particle Systems Characterization*, *12*(3), 148–157. https://doi.org/10.1002/ppsc.19950120307

Laurent, S., Forge, D., Port, M., Roch, A., Robic, C., Vander Elst, L., & Muller, R. N. (2010). Magnetic Iron Oxide Nanoparticles: Synthesis, Stabilization, Vectorization, Physicochemical Characterizations, and Biological Applications. *Chemical Reviews*, *110*(4), 2574–2574. https://doi.org/10.1021/cr900197g

Le Ouay, B., & Stellacci, F. (2015). Antibacterial activity of silver nanoparticles: A surface science insight. *Nano Today*, *10*(3), 339–354. https://doi.org/10.1016/j.nantod.2015.04.002

Lee, H.-Y., Li, Z., Chen, K., Hsu, A. R., Xu, C., Xie, J., Sun, S., & Chen, X. (2008). PET/MRI Dual-Modality Tumor Imaging Using Arginine-Glycine-Aspartic (RGD)–Conjugated Radiolabeled Iron Oxide Nanoparticles. *Journal of Nuclear Medicine*, *49*(8), 1371–1379. https://doi.org/10.2967/jnumed.108.051243

Lee, J.-H., Lim, J.-M., Velmurugan, P., Park, Y.-J., Park, Y.-J., Bang, K.-S., & Oh, B.-T. (2016). Photobiologic-mediated fabrication of silver nanoparticles with antibacterial activity. *Journal of Photochemistry and Photobiology B: Biology*, *162*, 93–99. https://doi.org/10.1016/j.jphotobiol.2016.06.029

Leung, A. B., Suh, K. I., & Ansari, R. R. (2006). Particle-size and velocity measurements in flowing conditions using dynamic light scattering. *Applied Optics*, *45*(10), 2186–2190. https://doi.org/10.1364/ao.45.002186

Li, M., Gou, H., Al-Ogaidi, I., & Wu, N. (2013). Nanostructured Sensors for Detection of Heavy Metals: A Review. *ACS Sustainable Chemistry & Engineering*, *1*(7), 713–723. https://doi.org/10.1021/sc400019a

Li, Y., Wang, J., Liu, Y., Luo, X., Lei, W., & Xie, L. (2020). Antiviral and virucidal effects of curcumin on transmissible gastroenteritis virus in vitro. *The Journal of General Virology*, *101*(10), 1079–1084. https://doi.org/10.1099/jgv.0.001466

Lidén, G. (2011). The European Commission Tries to Define Nanomaterials. *The Annals of Occupational Hygiene*, *55*(1), 1–5. https://doi.org/10.1093/annhyg/meq092

Lin, P.-C., Lin, S., Wang, P. C., & Sridhar, R. (2014a). Techniques for physicochemical characterization of nanomaterials. *Biotechnology Advances*, *32*(4), 711–726. https://doi.org/10.1016/j.biotechadv.2013.11.006

Lin, P.-C., Lin, S., Wang, P. C., & Sridhar, R. (2014b). Techniques for physicochemical characterization of nanomaterials. *Biotechnology Advances*, *32*(4), 711–726. https://doi.org/10.1016/j.biotechadv.2013.11.006

Lin, P.-C., Lin, S., Wang, P. C., & Sridhar, R. (2014c). Techniques for physicochemical characterization of nanomaterials. *Biotechnology Advances*, *32*(4), 711–726. https://doi.org/10.1016/j.biotechadv.2013.11.006

Link, S., & El-Sayed, M. A. (2003). Optical Properties and Ultrafast Dynamics of Metallic Nanocrystals. *Annual Review of Physical Chemistry*, *54*(1), 331–366. https://doi.org/10.1146/annurev.physchem.54.011002.103759

Litvin, V. A., & Minaev, B. F. (2013). Spectroscopy study of silver nanoparticles fabrication using synthetic humic substances and their antimicrobial activity. *Spectrochimica Acta. Part A, Molecular and Biomolecular Spectroscopy*, *108*, 115–122. https://doi.org/10.1016/j.saa.2013.01.049

Liu, H., & Webster, T. J. (2007). Nanomedicine for implants: A review of studies and necessary experimental tools. *Biomaterials*, *28*(2), 354–369. https://doi.org/10.1016/j.biomaterials.2006.08.049

Liu, Y., Liang, P., & Guo, L. (2005). Nanometer titanium dioxide immobilized on silica gel as sorbent for preconcentration of metal ions prior to their determination by inductively coupled plasma atomic emission spectrometry. *Talanta*, *68*(1), 25–30. https://doi.org/10.1016/j.talanta.2005.04.035

Loiseau, A., Asila, Boitel-Aullen, G., Lam, M., Salmain, & Boujday, S. (2019). Silver-Based Plasmonic Nanoparticles for and Their Use in Biosensing. *Biosensors*, *9*, 78. https://doi.org/10.3390/bios9020078

Lok, C.-N., Ho, C.-M., Chen, R., He, Q.-Y., Yu, W.-Y., Sun, H., Tam, P. K.-H., Chiu, J.-F., & Che, C.-M. (2006). Proteomic Analysis of the Mode of Antibacterial Action of Silver Nanoparticles. *Journal of Proteome Research*, *5*(4), 916–924. https://doi.org/10.1021/pr0504079

Ma, E. (2003). Controlling plastic instability. *Nature Materials*, *2*(1), 7–8. https://doi.org/10.1038/nmat797

Madivoli, E. S., Kareru, P. G., Gachanja, A. N., Mugo, S. M., Makhanu, D. S., Wanakai, S. I., & Gavamukulya, Y. (2020). Facile Synthesis of Silver Nanoparticles Using Lantana trifolia Aqueous Extracts and Their Antibacterial Activity. *Journal of Inorganic and Organometallic Polymers and Materials*, *30*(8), 2842–2850. https://doi.org/10.1007/s10904-019-01432-5

Mallick, K., Witcomb, M., & Scurrell, M. (2006). Silver nanoparticle catalysed redox reaction: An electron relay effect. *Materials Chemistry and Physics*, *97*(2), 283–287. https://doi.org/10.1016/j.matchemphys.2005.08.011

Manikandan, R., Manikandan, B., Raman, T., Arunagirinathan, K., Prabhu, N. M., Jothi Basu, M., Perumal, M., Palanisamy, S., & Munusamy, A. (2015). Biosynthesis of silver nanoparticles using ethanolic petals extract of Rosa indica and characterization of its antibacterial, anticancer and anti-inflammatory activities. *Spectrochimica Acta. Part A, Molecular and Biomolecular Spectroscopy*, *138*, 120–129. https://doi.org/10.1016/j.saa.2014.10.043

Manna, A., Imae, T., Aoi, K., Okada, M., & Yogo, T. (2001). Synthesis of Dendrimer-Passivated Noble Metal Nanoparticles in a Polar Medium: Comparison of Size

between Silver and Gold Particles. *Chemistry of Materials*, *13*(5), 1674–1681. https://doi.org/10.1021/cm000416b

Mäntele, W. G., Wollenweber, A. M., Nabedryk, E., & Breton, J. (1988). Infrared spectroelectrochemistry of bacteriochlorophylls and bacteriopheophytins: Implications for the binding of the pigments in the reaction center from photosynthetic bacteria. *Proceedings of the National Academy of Sciences*, *85*(22), 8468–8472. https://doi.org/10.1073/pnas.85.22.8468

Marimuthu, S., Antonisamy, A. J., Malayandi, S., Rajendran, K., Tsai, P.-C., Pugazhendhi, A., & Ponnusamy, V. K. (2020). Silver nanoparticles in dye effluent treatment: A review on synthesis, treatment methods, mechanisms, photocatalytic degradation, toxic effects and mitigation of toxicity. *Journal of Photochemistry and Photobiology B: Biology*, *205*, 111823. https://doi.org/10.1016/j.jphotobiol.2020.111823

Medley, C. D., Smith, J. E., Tang, Z., Wu, Y., Bamrungsap, S., & Tan, W. (2008). Gold Nanoparticle-Based Colorimetric Assay for the Direct Detection of Cancerous Cells. *Analytical Chemistry*, *80*(4), 1067–1072. https://doi.org/10.1021/ac702037y

Meyers, M. A., Mishra, A., & Benson, D. J. (2006). Mechanical properties of nanocrystalline materials. *Progress in Materials Science*, *51*(4), 427–556. https://doi.org/10.1016/j.pmatsci.2005.08.003

Mohanpuria, P., Rana, N. K., & Yadav, S. K. (2008). Biosynthesis of nanoparticles: Technological concepts and future applications. *Journal of Nanoparticle Research*, *10*(3), 507–517. https://doi.org/10.1007/s11051-007-9275-x

Morris, T., & Szulczewski, G. (2002). A Spectroscopic Ellipsometry, Surface Plasmon Resonance, and X-ray Photoelectron Spectroscopy Study of Hg Adsorption on Gold Surfaces. *Langmuir*, *18*(6), 2260–2264. https://doi.org/10.1021/la011525n

Moura, D., Souza, M. T., Liverani, L., Rella, G., Luz, G. M., Mano, J. F., & Boccaccini, A. R. (2017). Development of a bioactive glass-polymer composite for wound

healing applications. *Materials Science and Engineering: C*, *76*, 224–232. https://doi.org/10.1016/j.msec.2017.03.037

MubarakAli, D., Thajuddin, N., Jeganathan, K., & Gunasekaran, M. (2011). Plant extract mediated synthesis of silver and gold nanoparticles and its antibacterial activity against clinically isolated pathogens. *Colloids and Surfaces. B, Biointerfaces*, *85*(2), 360–365. https://doi.org/10.1016/j.colsurfb.2011.03.009

Mulvaney, P. (1996). Surface Plasmon Spectroscopy of Nanosized Metal Particles. *Langmuir*, *12*(3), 788–800. https://doi.org/10.1021/la9502711

Mulyaningsih, R. D., Pratiwi, R., & Hasanah, A. N. (2023). An Update on the Use of Natural Pigments and Pigment Nanoparticle Adducts for Metal Detection Based on Colour Response. *Biosensors*, *13*(5), 554. https://doi.org/10.3390/bios13050554

Murdock, R. C., Braydich-Stolle, L., Schrand, A. M., Schlager, J. J., & Hussain, S. M. (2008). Characterization of Nanomaterial Dispersion in Solution Prior to In Vitro Exposure Using Dynamic Light Scattering Technique. *Toxicological Sciences*, *101*(2), 239–253. https://doi.org/10.1093/toxsci/kfm240

Nath, B., Das, B., Kalita, P., & Basumatary, S. (2019). Waste to value addition: Utilization of waste Brassica nigra plant derived novel green heterogeneous base catalyst for effective synthesis of biodiesel. *Journal of Cleaner Production*, *239*, 118112. https://doi.org/10.1016/j.jclepro.2019.118112

Niikura, K., Nagakawa, K., Ohtake, N., Suzuki, T., Matsuo, Y., Sawa, H., & Ijiro, K. (2009). Gold Nanoparticle Arrangement on Viral Particles through Carbohydrate Recognition: A Non-Cross-Linking Approach to Optical Virus Detection. *Bioconjugate Chemistry*, *20*(10), 1848–1852. https://doi.org/10.1021/bc900255x

Noginov, M. A., Zhu, G., Bahoura, M., Adegoke, J., Small, C., Ritzo, B. A., Drachev, V. P., & Shalaev, V. M. (2007). The effect of gain and absorption on surface plasmons in metal nanoparticles. *Applied Physics B*, *86*(3), 455–460. https://doi.org/10.1007/s00340-006-2401-0

Olteanu, N. L., Rogozea, E. A., Popescu, S. A., Petcu, A. R., Lazăr, C. A., Meghea, A., & Mihaly, M. (2016). "One-pot" synthesis of Au–ZnO–SiO2 nanostructures for sunlight photodegradation. *Journal of Molecular Catalysis A: Chemical*, *414*, 148–159. https://doi.org/10.1016/j.molcata.2016.01.007

Ouda, S. M. (2014). Some Nanoparticles Effects on *Proteus sp.* And *Klebsiella* Sp. Isolated from Water. *American Journal of Infectious Diseases and Microbiology*, *2*(1), Article 1. https://doi.org/10.12691/ajidm-2-1-2

Panigrahi, S., Kundu, S., Ghosh, S., Nath, S., & Pal, T. (2004). General method of synthesis for metal nanoparticles. *Journal of Nanoparticle Research*, *6*(4), 411–414. https://doi.org/10.1007/s11051-004-6575-2

Pavlidou, S., & Papaspyrides, C. D. (2008). A review on polymer–layered silicate nanocomposites. *Progress in Polymer Science*, *33*(12), 1119–1198. https://doi.org/10.1016/j.progpolymsci.2008.07.008

Perevedentseva, E. V., F.y, S., T.h, S., Y.c, L., C.l, C., Karmenyan, A. V., Priezzhev, A. V., & Lugovtsov, A. E. (2010). Laser-optical investigation of the effect of diamond nanoparticles on the structure and functional properties of proteins. *Quantum Electronics*, *40*(12), 1089. https://doi.org/10.1070/QE2010v040n12ABEH014507

Phull, A.-R., Abbas, Q., Ali, A., Raza, H., kim, S. J., Zia, M., & Haq, I. (2016). Antioxidant, cytotoxic and antimicrobial activities of green synthesized silver nanoparticles from crude extract of Bergenia ciliata. *Future Journal of Pharmaceutical Sciences*, *2*(1), 31–36. https://doi.org/10.1016/j.fjps.2016.03.001

Pissuwan, D., Valenzuela, S. M., & Cortie, M. B. (2006). Therapeutic possibilities of plasmonically heated gold nanoparticles. *Trends in Biotechnology*, *24*(2), 62–67. https://doi.org/10.1016/j.tibtech.2005.12.004

Prakash, P., Gnanaprakasam, P., Emmanuel, R., Arokiyaraj, S., & Saravanan, M. (2013). Green synthesis of silver nanoparticles from leaf extract of Mimusops elengi, Linn. For enhanced antibacterial activity against multi drug resistant

clinical isolates. *Colloids and Surfaces B: Biointerfaces*, *108*, 255–259. https://doi.org/10.1016/j.colsurfb.2013.03.017

Prasad, S., Gupta, S. C., Tyagi, A. K., & Aggarwal, B. B. (2014). Curcumin, a component of golden spice: From bedside to bench and back. *Biotechnology Advances*, *32*(6), 1053–1064. https://doi.org/10.1016/j.biotechadv.2014.04.004

Puente, C., Gómez, I., Kharisov, B., & López, I. (2019). Selective colorimetric sensing of Zn(II) ions using green-synthesized silver nanoparticles: Ficus benjamina extract as reducing and stabilizing agent. *Materials Research Bulletin*, *112*, 1–8. https://doi.org/10.1016/j.materresbull.2018.11.045

Qin, M., Wang, X., Hu, Y., Ding, X., Song, Y., Li, M., Vasilakos, P., Nenes, A., & Russell, A. G. (2018). Simulating Biogenic Secondary Organic Aerosol During Summertime in China. *Journal of Geophysical Research: Atmospheres*, *123*(19), 11,100-11,119. https://doi.org/10.1029/2018JD029185

Rai, M., Yadav, A., & Gade, A. (2008). CRC 675—Current Trends in Phytosynthesis of Metal Nanoparticles. *Critical Reviews in Biotechnology*, *28*(4), 277–284. https://doi.org/10.1080/07388550802368903

Rajkumari, K., Das, D., Pathak, G., & Rokhum, S. L. (2019). Waste-to-useful: A biowaste-derived heterogeneous catalyst for a green and sustainable Henry reaction. *New Journal of Chemistry*, *43*(5), 2134–2140. https://doi.org/10.1039/C8NJ05029E

Ramsden, J. J., & Tóth-Boconádi, R. (1990). Pulsed photoelectrochemistry of titanium dioxide. *Journal of the Chemical Society, Faraday Transactions*, *86*(9), 1527–1533. https://doi.org/10.1039/FT9908601527

Rawat, R. S. (2015). Dense Plasma Focus—From Alternative Fusion Source to Versatile High Energy Density Plasma Source for Plasma Nanotechnology. *Journal of Physics: Conference Series*, *591*(1), 012021. https://doi.org/10.1088/1742-6596/591/1/012021

Rogozea, E. A., Olteanu, N. L., Petcu, A. R., Lazar, C. A., Meghea, A., & Mihaly, M. (2016). Extension of optical properties of ZnO/SiO2 materials induced by

incorporation of Au or NiO nanoparticles. *Optical Materials*, *56*, 45–48. https://doi.org/10.1016/j.optmat.2015.12.020

Roy, K., Sarkar, C. K., & Ghosh, C. K. (2015). Plant-mediated synthesis of silver nanoparticles using parsley (Petroselinum crispum) leaf extract: Spectral analysis of the particles and antibacterial study. *Applied Nanoscience*, *5*(8), 945–951. https://doi.org/10.1007/s13204-014-0393-3

Saifuddin, N., Wong, C. W., & Yasumira, A. A. N. (NaN/NaN/NaN). Rapid Biosynthesis of Silver Nanoparticles Using Culture Supernatant of Bacteria with Microwave Irradiation. *Journal of Chemistry*, *6*, 61–70. https://doi.org/10.1155/2009/734264

Sankar, R., Rahman, P. K. S. M., Varunkumar, K., Anusha, C., Kalaiarasi, A., Shivashangari, K. S., & Ravikumar, V. (2017). Facile synthesis of Curcuma longa tuber powder engineered metal nanoparticles for bioimaging applications. *Journal of Molecular Structure*, *1129*, 8–16. https://doi.org/10.1016/j.molstruc.2016.09.054

Sapsford, K. E., Tyner, K. M., Dair, B. J., Deschamps, J. R., & Medintz, I. L. (2011). Analyzing Nanomaterial Bioconjugates: A Review of Current and Emerging Purification and Characterization Techniques. *Analytical Chemistry*, *83*(12), 4453–4488. https://doi.org/10.1021/ac200853a

Sastry, M., Mayya, K. S., & Bandyopadhyay, K. (1997). PH Dependent changes in the optical properties of carboxylic acid derivatized silver colloidal particles. *Colloids and Surfaces A: Physicochemical and Engineering Aspects*, *127*(1), 221–228. https://doi.org/10.1016/S0927-7757(97)00087-3

Sastry, M., Patil, V., & Sainkar, S. R. (1998). Electrostatically Controlled Diffusion of Carboxylic Acid Derivatized Silver Colloidal Particles in Thermally Evaporated Fatty Amine Films. *The Journal of Physical Chemistry B*, *102*(8), 1404–1410. https://doi.org/10.1021/jp9719873

Sathishkumar, M., Sneha, K., & Yun, Y.-S. (2010). Immobilization of silver nanoparticles synthesized using Curcuma longa tuber powder and extract on

cotton cloth for bactericidal activity. *Bioresource Technology*, *101*(20), 7958–7965. https://doi.org/10.1016/j.biortech.2010.05.051

Šebesta, M., Vojtková, H., Cyprichová, V., Ingle, A. P., Urík, M., & Kolenčík, M. (2023). Mycosynthesis of Metal-Containing Nanoparticles—Synthesis by Ascomycetes and Basidiomycetes and Their Application. *International Journal of Molecular Sciences*, *24*(1), Article 1. https://doi.org/10.3390/ijms24010304

Selvi, N. T., Navamathavan, R., Kim, H. Y., & Nirmala, R. (2019). Autoclave Mediated Synthesis of Silver Nanoparticles Using Aqueous Extract of Canna indica L. Rhizome and Evaluation of Its Antimicrobial Activity. *Macromolecular Research*, *27*(11), 1155–1160. https://doi.org/10.1007/s13233-019-7159-4

Shameli, K., Ahmad, M. B., Shabanzadeh, P., Jaffar Al-Mulla, E. A., Zamanian, A., Abdollahi, Y., Jazayeri, S. D., Eili, M., Jalilian, F. A., & Haroun, R. Z. (2014). Effect of Curcuma longa tuber powder extract on size of silver nanoparticles prepared by green method. *Research on Chemical Intermediates*, *40*(3), 1313–1325. https://doi.org/10.1007/s11164-013-1040-4

Shameli, K., Ahmad, M. B., Zamanian, A., Sangpour, P., Shabanzadeh, P., Abdollahi, Y., & Zargar, M. (2012). Green biosynthesis of silver nanoparticles using Curcuma longa tuber powder. *International Journal of Nanomedicine*, *7*, 5603–5610. https://doi.org/10.2147/IJN.S36786

Shang, L., Wang, Y., Jiang, J., & Dong, S. (2007). pH-Dependent Protein Conformational Changes in Albumin:Gold Nanoparticle Bioconjugates: A Spectroscopic Study. *Langmuir*, *23*(5), 2714–2721. https://doi.org/10.1021/la062064e

Sharma, G., Nam, J.-S., Sharma, A. R., & Lee, S.-S. (2018). Antimicrobial Potential of Silver Nanoparticles Synthesized Using Medicinal Herb Coptidis rhizome. *Molecules*, *23*(9), Article 9. https://doi.org/10.3390/molecules23092268

Shivaji, S., Madhu, S., & Singh, S. (2011). Extracellular synthesis of antibacterial silver nanoparticles using psychrophilic bacteria. *Process Biochemistry*, *46*(9), 1800–1807. https://doi.org/10.1016/j.procbio.2011.06.008

Siddiqui, M., Al-whaibi, M., Mohammad, F., & Al-Khaishany, M. (2015). Role of Nanoparticles in Plants. In *Nanotechnology and Plant Sciences: Nanoparticles and Their Impact on Plants* (pp. 19–35). https://doi.org/10.1007/978-3-319-14502-0_2

Silver, S. (2003). Bacterial silver resistance: Molecular biology and uses and misuses of silver compounds. *FEMS Microbiology Reviews*, *27*(2–3), 341–353. https://doi.org/10.1016/S0168-6445(03)00047-0

Singh, D., Rathod, V., Ninganagouda, S., Hiremath, J., Singh, A. K., & Mathew, J. (2014). Optimization and Characterization of Silver Nanoparticle by Endophytic Fungi *Penicillium* sp. Isolated from *Curcuma longa* (Turmeric) and Application Studies against MDR *E. coli* and *S. aureus*. *Bioinorganic Chemistry and Applications*, *2014*, e408021. https://doi.org/10.1155/2014/408021

Sinha Ray, S., & Okamoto, M. (2003). Polymer/layered silicate nanocomposites: A review from preparation to processing. *Progress in Polymer Science*, *28*(11), 1539–1641. https://doi.org/10.1016/j.progpolymsci.2003.08.002

Song, J. Y., & Kim, B. S. (2009). Rapid biological synthesis of silver nanoparticles using plant leaf extracts. *Bioprocess and Biosystems Engineering*, *32*(1), 79–84. https://doi.org/10.1007/s00449-008-0224-6

Stepanov, A. L. (2004). Optical properties of metal nanoparticles synthesized in a polymer by ion implantation: A review. *Technical Physics*, *49*(2), 143–153. https://doi.org/10.1134/1.1648948

Sumitha, S., Vasanthi, S., Shalini, S., Chinni, S. V., Gopinath, S. C. B., Anbu, P., Bahari, M. B., Harish, R., Kathiresan, S., & Ravichandran, V. (2018). Phyto-Mediated Photo Catalysed Green Synthesis of Silver Nanoparticles Using Durio Zibethinus Seed Extract: Antimicrobial and Cytotoxic Activity and Photocatalytic Applications. *Molecules*, *23*(12), Article 12. https://doi.org/10.3390/molecules23123311

Taleb, A., Petit, C., & Pileni, M. P. (1998). Optical Properties of Self-Assembled 2D and 3D Superlattices of Silver Nanoparticles. *The Journal of Physical Chemistry B*, *102*(12), 2214–2220. https://doi.org/10.1021/jp972807s

Tang, Y., He, F., Yu, M., Feng, F., An, L., Sun, H., Wang, S., Li, Y., & Zhu, D. (2006). A Reversible and Highly Selective Fluorescent Sensor for Mercury(II) Using Poly(thiophene)s that Contain Thymine Moieties. *Macromolecular Rapid Communications*, *27*(6), 389–392. https://doi.org/10.1002/marc.200500837

Todescato, F., Fortunati, I., Minotto, A., Signorini, R., Jasieniak, J. J., & Bozio, R. (2016). Engineering of Semiconductor Nanocrystals for Light Emitting Applications. *Materials*, *9*(8), Article 8. https://doi.org/10.3390/ma9080672

Tomaszewska, E., Soliwoda, K., Kadziola, K., Tkacz-Szczesna, B., Celichowski, G., Cichomski, M., Szmaja, W., & Grobelny, J. (2013). Detection Limits of DLS and UV-Vis Spectroscopy in Characterization of Polydisperse Nanoparticles Colloids. *Journal of Nanomaterials*, *2013*, e313081. https://doi.org/10.1155/2013/313081

Uzawa, H., Ohga, K., Shinozaki, Y., Ohsawa, I., Nagatsuka, T., Seto, Y., & Nishida, Y. (2008). A novel sugar-probe biosensor for the deadly plant proteinous toxin, ricin. *Biosensors and Bioelectronics*, *24*(4), 923–927. https://doi.org/10.1016/j.bios.2008.07.049

Vaia, R. A., & Liu, W. (2002). X-ray powder diffraction of polymer/layered silicate nanocomposites: Model and practice. *Journal of Polymer Science Part B: Polymer Physics*, *40*(15), 1590–1600. https://doi.org/10.1002/polb.10214

Vanaja, M., Paulkumar, K., Baburaja, M., Rajeshkumar, S., Gnanajobitha, G., Malarkodi, C., Sivakavinesan, M., & Annadurai, G. (2014). Degradation of Methylene Blue Using Biologically Synthesized Silver Nanoparticles. *Bioinorganic Chemistry and Applications*, *2014*, e742346. https://doi.org/10.1155/2014/742346

Vanlalveni, C., Lallianrawna, S., Biswas, A., Selvaraj, M., Changmai, B., & Rokhum, S. L. (2021). Green synthesis of silver nanoparticles using plant extracts and their antimicrobial activities: A review of recent literature. *RSC Advances*, *11*(5), 2804–2837. https://doi.org/10.1039/D0RA09941D

Verma, A., & Mehata, M. S. (2016). Controllable synthesis of silver nanoparticles using Neem leaves and their antimicrobial activity. *Journal of Radiation Research*

and Applied Sciences, *9*(1), 109–115. https://doi.org/10.1016/j.jrras.2015.11.001

Vigneshwaran, N., Ashtaputre, N. M., Varadarajan, P. V., Nachane, R. P., Paralikar, K. M., & Balasubramanya, R. H. (2007). Biological synthesis of silver nanoparticles using the fungus Aspergillus flavus. *Materials Letters*, *61*(6), 1413–1418. https://doi.org/10.1016/j.matlet.2006.07.042

Vijayan, S. R., Santhiyagu, P., Ramasamy, R., Arivalagan, P., Kumar, G., Ethiraj, K., & Ramaswamy, B. R. (2016). Seaweeds: A resource for marine bionanotechnology. *Enzyme and Microbial Technology*, *95*, 45–57. https://doi.org/10.1016/j.enzmictec.2016.06.009

Vogel, R., & Siebert, F. (2000). Vibrational spectroscopy as a tool for probing protein function. *Current Opinion in Chemical Biology*, *4*(5), 518–523. https://doi.org/10.1016/S1367-5931(00)00125-3

Wang, P., Huang, B., Zhang, X., Qin, X., Dai, Y., Jin, H., Wei, J., & Whangbo, M.-H. (2008). Composite Semiconductor H2WO4·H2O/AgCl as an Efficient and Stable Photocatalyst under Visible Light. *Chemistry – A European Journal*, *14*(34), 10543–10546. https://doi.org/10.1002/chem.200801733

Wang, Q., Kim, D., Dionysiou, D. D., Sorial, G. A., & Timberlake, D. (2004). Sources and remediation for mercury contamination in aquatic systems—A literature review. *Environmental Pollution*, *131*(2), 323–336. https://doi.org/10.1016/j.envpol.2004.01.010

Wang, Z. L. (2000). Transmission Electron Microscopy of Shape-Controlled Nanocrystals and Their Assemblies. *The Journal of Physical Chemistry B*, *104*(6), 1153–1175. https://doi.org/10.1021/jp993593c

Wen, C.-C., Kuo, Y.-H., Jan, J.-T., Liang, P.-H., Wang, S.-Y., Liu, H.-G., Lee, C.-K., Chang, S.-T., Kuo, C.-J., Lee, S.-S., Hou, C.-C., Hsiao, P.-W., Chien, S.-C., Shyur, L.-F., & Yang, N.-S. (2007). Specific Plant Terpenoids and Lignoids Possess Potent Antiviral Activities against Severe Acute Respiratory Syndrome Coronavirus. *Journal of Medicinal Chemistry*, *50*(17), 4087–4095. https://doi.org/10.1021/jm070295s

Williams, D. B., & Carter, C. B. (1996). The Transmission Electron Microscope. In D. B. Williams & C. B. Carter (Eds.), *Transmission Electron Microscopy: A Textbook for Materials Science* (pp. 3–17). Springer US. https://doi.org/10.1007/978-1-4757-2519-3_1

Xiao, N., & Yu, C. (2010). Rapid-Response and Highly Sensitive Noncross-Linking Colorimetric Nitrite Sensor Using 4-Aminothiophenol Modified Gold Nanorods. *Analytical Chemistry*, *82*(9), 3659–3663. https://doi.org/10.1021/ac902924p

Yazdian, N., Karimzadeh, F., & Enayati, M. H. (2013). In-situ fabrication of Al3V/Al2O3 nanocomposite through mechanochemical synthesis and evaluation of its mechanism. *Advanced Powder Technology*, *24*(1), 106–112. https://doi.org/10.1016/j.apt.2012.03.004

Yoosaf, K., Ipe, B. I., Suresh, C. H., & Thomas, K. G. (2007). In Situ Synthesis of Metal Nanoparticles and Selective Naked-Eye Detection of Lead Ions from Aqueous Media. *The Journal of Physical Chemistry C*, *111*(34), 12839–12847. https://doi.org/10.1021/jp073923q

Yuan, X., Setyawati, M. I., Tan, A. S., Ong, C. N., Leong, D. T., & Xie, J. (2013). Highly luminescent silver nanoclusters with tunable emissions: Cyclic reduction–decomposition synthesis and antimicrobial properties. *NPG Asia Materials*, *5*(2), Article 2. https://doi.org/10.1038/am.2013.3

Zahir, F., Rizwi, S. J., Haq, S. K., & Khan, R. H. (2005). Low dose mercury toxicity and human health. *Environmental Toxicology and Pharmacology*, *20*(2), 351–360. https://doi.org/10.1016/j.etap.2005.03.007

Zanetti-Ramos, B. G., Fritzen-Garcia, M. B., de Oliveira, C. S., Pasa, A. A., Soldi, V., Borsali, R., & Creczynski-Pasa, T. B. (2009). Dynamic light scattering and atomic force microscopy techniques for size determination of polyurethane nanoparticles. *Materials Science and Engineering: C*, *29*(2), 638–640. https://doi.org/10.1016/j.msec.2008.10.040

Zargar, M., Hamid, A. A., Bakar, F. A., Shamsudin, M. N., Shameli, K., Jahanshiri, F., & Farahani, F. (2011). Green Synthesis and Antibacterial Effect of Silver

Nanoparticles Using Vitex Negundo L. *Molecules*, *16*(8), Article 8. https://doi.org/10.3390/molecules16086667

Zawrah, M. F., Zayed, H. A., Essawy, R. A., Nassar, A. H., & Taha, M. A. (2013). Preparation by mechanical alloying, characterization and sintering of Cu–20wt.% Al2O3 nanocomposites. *Materials & Design (1980-2015)*, *46*, 485–490. https://doi.org/10.1016/j.matdes.2012.10.032

Žerjav, G., Albreht, A., Vovk, I., & Pintar, A. (2020). Revisiting terephthalic acid and coumarin as probes for photoluminescent determination of hydroxyl radical formation rate in heterogeneous photocatalysis. *Applied Catalysis A: General*, *598*, 117566. https://doi.org/10.1016/j.apcata.2020.117566

Zhang, J. F., Park, M., Ren, W. X., Kim, Y., Kim, S. J., Jung, J. H., & Kim, J. S. (2011). A pellet-type optical nanomaterial of silica-based naphthalimide–DPA–Cu(II) complexes: Recyclable fluorescence detection of pyrophosphate. *Chemical Communications*, *47*(12), 3568–3570. https://doi.org/10.1039/C1CC00021G

Zhang, X.-F., Liu, Z.-G., Shen, W., & Gurunathan, S. (2016). Silver Nanoparticles: Synthesis, Characterization, Properties, Applications, and Therapeutic Approaches. *International Journal of Molecular Sciences*, *17*(9), Article 9. https://doi.org/10.3390/ijms17091534

Zhao, G., & Stevens, S. E. (1998). Multiple parameters for the comprehensive evaluation of the susceptibility of Escherichia coli to the silver ion. *Biometals*, *11*(1), 27–32. https://doi.org/10.1023/A:1009253223055

Zhao, W., Brook, M. A., & Li, Y. (2008). Design of Gold Nanoparticle-Based Colorimetric Biosensing Assays. *ChemBioChem*, *9*(15), 2363–2371. https://doi.org/10.1002/cbic.200800282

Zhao, X.-Z., Jiang, T., Wang, L., Yang, H., Zhang, S., & Zhou, P. (2010). Interaction of curcumin with Zn(II) and Cu(II) ions based on experiment and theoretical calculation. *Journal of Molecular Structure*, *984*(1), 316–325. https://doi.org/10.1016/j.molstruc.2010.09.049

Zheng, W., Aschner, M., & Ghersi-Egea, J.-F. (2003). Brain barrier systems: A new frontier in metal neurotoxicological research. *Toxicology and Applied Pharmacology*, *192*(1), 1–11. https://doi.org/10.1016/S0041-008X(03)00251-5

Zietz, B. P., Dieter, H. H., Lakomek, M., Schneider, H., Keßler-Gaedtke, B., & Dunkelberg, H. (2003). Epidemiological investigation on chronic copper toxicity to children exposed via the public drinking water supply. *Science of The Total Environment*, *302*(1), 127–144. https://doi.org/10.1016/S0048-9697(02)00399-6

APPENDIX

Calculation of Amount of $AgNO_3$ required:

Molecular weight = 169.873 g/mol

Amount of $AgNO_3$ required to prepare 50 mM $AgNO_3$

$$\text{Weight taken} = \frac{\text{Molarity} \times \text{Molecular weight} \times \text{Volume of solution}}{1000}$$

= (50 X 10^{-3} X 169.873 X 500) / 1000

= 4.246825 g ~ 4.247 g in 500 mL distilled water

Dilution of 50 mM $AgNO_3$ to prepare 500 mL of $AgNO_3$

Volume of 50 mM $AgNO_3$ required

= (Final Molarity X Final volume) /Initial Molarity

= (1 mM X 500 mL) / 50 mM

= 10 mL

Amount of following metal salt required to prepare 100 mL of 0.01 M were calculated by using above formula as follows:

$CrCl_3$. $6H_2O$

Weight required = (0.01 X 266.45 X 100) / 1000 = 0.266 g

$ZnSO_4.7H_2O$

Weight required = (0.01 X 287.54 X 100) / 1000 = 0.288 g

$HgCl_2$

Weight required = (0.01 X 271.50 X 100) / 1000 = 0.272 g

As_2O_3

Weight required = (0.01 X 197.84 X 100) / 1000 = 0.198 g

$BaCl_2.2H_2O$

Weight required = (0.01 X 244.21 X 100) / 1000 = 0.244 g

$Ni(NO)_3.6H_2O$

Weight required = (0.01 X 290.81 X 100) / 1000 = 0.291 g

$CuCl_2.2H_2O$

Weight required = (0.01 X 170.48 X 100) / 1000 = 0.170 g

$MnSO_4$

Weight required = (0.01 X 169.06 X 100) / 1000 = 0.169 g

Photographs of some important instruments

Centriuge

UV-Vis Spectrophotometer

Magnetic Stirrer

Photographs while performing the experiment

During collection of nanoparticles

Taking the absorbance in UV-Visible spectrophotometer

Maintaining the temperature in magnetic stirrir